

Montclair State University

Montclair State University Digital Commons

Theses, Dissertations and Culminating Projects

5-2017

Preliminary Investigation and Sequence of the Hyaluronidase Gene in the Venom of the Atlantic Sea Nettle (*Chrysaora quinquecirrha*)

Zachary A. Cropley

Follow this and additional works at: <https://digitalcommons.montclair.edu/etd>

 Part of the [Biology Commons](#)

Abstract

Jellyfish cnidocysts contain many different venom proteins, each with unique functions that combine synergistically to achieve a more robust and toxic fluid. One of these proteins is hyaluronidase (EC 3.2.1.35), an enzyme that breaks down hyaluronic acid, which is commonly found in the extracellular matrix of many multicellular organisms. Due to its wide application, this enzyme is also found in the venom of many arthropod and reptile families. Putatively, hyaluronidase aids in the dispersion of the other venom proteins as it perforates the matrix in the target tissue. This activity has been detected in *Chrysaora quinquecirrha* cnidocysts, but the gene encoding hyaluronidase has yet to be identified or sequenced in full. Preliminary analysis of this protein shows high homology (67% homologous) to similar venom proteins found in another Cnidarian, *Hydra vulgaris*, which both conserve the active and secondary sites found in SPAM1, a protein found on the surface of mammalian sperm as well. *Chrysaora quinquecirrha*'s hyaluronidase was previously located in mRNA sequencing, which was then amplified from genomic DNA using primers designed off this sequence. While the primers were 674 base pairs (bp) apart in the RNA, amplification by PCR of *Chrysaora quinquecirrha* gDNA produced an amplicon of *ca.* 2300 bp. From the initial sequencing, additional primers were designed, which generated amplicons of 1100 bp. In aligning the sequences with each other and, using the original mRNA sequence as a scaffold, two introns were discovered and characterized, accounting for part of the size disparity between the RNA and DNA sequences. These represent the first introns identified and sequenced for this organism. The conservation of amino acid residues in the active site as well as several secondary sites in the putative protein support the conclusion that I have isolated a genomic clone of hyaluronidase. Additionally, the fact that hyaluronidase enzymatic activity was detected in extracts of purified cnidocysts isolated from *Chrysaora quinquecirrha* confirms that hyaluronidase is present in the venom of this jellyfish. The hyaluronidase protein found in other highly homologous species is longer than our present assembly encodes for, so

further extension of this sequence is necessary to elucidate the entire gene. Compared to the hyaluronidase-1 from *Hydra vulgaris*, which is 436 amino acids in length, I have generated a translation product of 280 amino acids, or *ca.* 64.2%.

MONTCLAIR STATE UNIVERSITY

PRELIMINARY INVESTIGATION AND SEQUENCE OF THE HYALURONIDASE GENE IN THE VENOM
OF THE ATLANTIC SEA NETTLE (*Chrysaora quinquecirrha*)

By

Zachary A. Cropley

A Master's Thesis Submitted to the Faculty of

Montclair State University

In Partial Fulfillment of the Requirements

For the Degree of

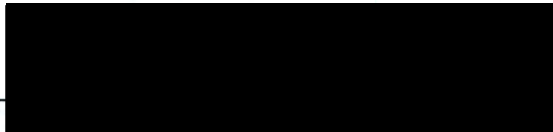
Master of Science


May 2017

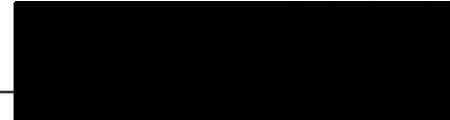
College of Science and Mathematics

Thesis Committee

Biology


Thesis Sponsor/ John J. Gaynor


Committee Member/ Vladislav Snitsarev


Committee Member/ Paul A. X. Bologna

PRELIMINARY INVESTIGATION AND SEQUENCE OF THE HYALURONIDASE GENE
IN THE VENOM OF THE ATLANTIC SEA NETTLE (*Chrysaora quinquecirrha*)

A THESIS

Submitted in partial fulfillment of the requirements

For the degree of Masters of Science in Molecular Biology

By

ZACHARY A. CROPLEY

Montclair State University

Montclair, NJ

2017

Table of Contents

List of Figures	iii
List of Tables	iv
Introduction	1
I. Cnidocysts	
1. Cnidocyst Biology	2
2. Cnidocyst Function	4
II. Cnidarian Toxins	
1. Anthozoan Toxins	6
2. Medusozoan Toxins	8
III. Hyaluronidase in <i>Chrysaora quinquecirrha</i>	10
IV. Hyaluronidase in Other Animals	11
V. Specific Aims	12
Materials and Methods	
I. <i>Chrysaora quinquecirrha</i> Transcriptome by RNA-Seq Analysis	13
II. DNA Isolation from <i>Chrysaora quinquecirrha</i>	15
III. Primer Design	18
IV. PCR Amplification	18
V. DNA Sequencing and Bioinformatic Analysis	19
VI. Hyaluronidase Assay	19
Results	
I. Evidence for Hyaluronidase Expression in the <i>Chrysaora quinquecirrha</i> Transcriptome	23

II.	Hyaluronidase Gene Structure from <i>Chrysaora quinquecirrha</i>	26
III.	Evidence for Introns in the Hyaluronidase Gene from <i>Chrysaora quinquecirrha</i>	35
IV.	Insertion Sequence within Intron	38
V.	Hyaluronidase Activity	40
VI.	Homology	41
Discussion		
I.	Evidence for Hyaluronidase Expression in the <i>Chrysaora quinquecirrha</i> Transcriptome	44
II.	Hyaluronidase Gene Structure from <i>Chrysaora quinquecirrha</i>	45
III.	Evidence for Introns in the Hyaluronidase Gene from <i>Chrysaora quinquecirrha</i>	46
IV.	Insertion Sequence within Intron	48
V.	Hyaluronidase Activity	48
VI.	Homology	50
Conclusion		51
Literature Cited		52

List of Figures

Figure 1. Estimation of gDNA (genomic DNA) size and integrity and test of DNase contamination of RNase A preparation	17
Figure 2. High concentration standard curve of bovine testicular hyaluronidase incubated for 45 minutes	22
Figure 3. Bovine testicular hyaluronidase standard curve for 7.5 µg/ml over time	22
Figure 4. Raw sequence read of Contig 20047 generated from <i>Chrysaora quinquecirrha</i> transcriptome	24
Figure 5. BLASTX results of the <i>Chrysaora quinquecirrha</i> RNA contig 20047 encoding the venom hyaluronidase gene	25
Figure 6. Putative hyaluronidase amino-acid sequence from <i>Chrysaora quinquecirrha</i> queried against <i>Hydra vulgaris</i> hyaluronidase	26
Figure 7. RNA seq with DNA annotations	27
Figure 8. DNA fragment sizes generated by HyalF/R and HyF/R from TR1 and 2	28
Figure 9. Standard curve generated by electrophoretic separation of HiLo ladder (Minnesota Molecular) fragments	29
Figure 10. <i>Chrysaora quinquecirrha</i> hyaluronidase primers used to amplify <i>Gonionemus vertens</i> hyaluronidase	30
Figure 11. Electropherograms of HyalR generated sequences prior to manual base call edits and gap deletions	31
Figure 12. Electropherograms of HyalR generated sequences after manual base call edits and gap deletions	32
Figure 13. Electropherograms of HyalF generated sequences prior to manual base call edits and gap deletions	32
Figure 14. Electropherograms of HyalF generated sequences after manual base call edits and gap deletions	33
Figure 15. Electropherograms of HyR and HyF generated sequences, homologous group 1 of 3	33
Figure 16. Electropherograms of HyR and HyF generated sequences, homologous group 2 of 3	34
Figure 17. Electropherograms of HyR and HyF generated sequences, homologous group 3 of 3	34
Figure 18. The first four sequences generated from the initial runs of each primer, HyalR, HyR and HyF from top to bottom	36

Figure 19. HyR-F exon alignment without any potential intron sequence. All 3 homologous groups are present	37
Figure 20. Alignment of homologous groups 1 and 2 together	39
Figure 21. Inverted repeats from the insertion sequence	40
Figure 22. Low concentration standard curves for bovine testicular hyaluronidase (Blue) and <i>Chrysaora quinquecirrha</i> cnidocyst hyaluronidase (Red) incubated for 45 minutes	41
Figure 23. Clustal alignment of <i>Chrysaora quinquecirrha</i> , <i>Hydra vulgaris</i> and several chordates' hyaluronidase	42
Figure 24. CLUSTAL Omega alignment of <i>Chrysaora quinquecirrha</i> , <i>Hydra vulgaris</i> and more closely related hyaluronidase genes	43

List of Tables

Table 1. List of primers used on TR1 and TR2	18
Table 2. Standard Layout for Hyaluronidase Assay	20

Introduction

The development of toxins has allowed some of the frailest and smallest organisms on earth to pose a threat to the largest multicellular organisms. Whether for predation or defense, toxins level the playing field between the simpler creatures and their predators or prey. While toxins come in many forms, most of them are proteinaceous. These proteins are often small, but bind cells in such a way as to hinder or kill the cell. While poisons and venoms both fall under this category, they are differentiated by their method of delivery. Poisons must be ingested, inhaled or otherwise internalized by the target. Venoms, on the other hand, are actively injected by the organism into its target, which can be either predator, prey or occasionally both. Proteinaceous venoms evolve along with the desired target, binding better to specific chemical moieties or protein channels in the host's membranes (Jouiaei et al., 2015). This coevolution drives venom to sustain or even enhance its potency over generations, allowing those with a proverbial head start to maintain exceptionally potent venom. It's no surprise then that the majority of the world's most venomous creatures are also some of the oldest animals. Venomous invertebrates, in particular aquatic ones, are some of the oldest and deadliest animals encountered by humans.

One of the oldest of these phyla, and one containing some of the most venomous creatures on earth, is Cnidaria. Cnidarians are ancient animals divided between two main subphyla, Medusozoa, commonly called jellyfish and Anthozoa, which include corals and anemone (Jouiaei et al., 2015). Both of these groups are structurally similar, but the anthozoa are sessile for their entire life whereas the medusozoa are only partially sessile. In this state, they are comparable to sea sponges, albeit often more predatory and with more complex cellular organization. Like sponges, cnidarians are very simple, lacking digestive or circulatory organs, relying on the thin layers of cells to diffuse the necessary nutrients from the water to intracellular layers. Unlike sponges however, cnidarians have rudimentary nervous systems and muscles since they are ambulatory and predatory in some cases. The tradeoff for these advances is that the cnidarians lose

the non-determinant layers of sponges that allow their cells to re-determine their function. As a result, the jellyfish and anemones have diminished ability to regenerate from being torn apart.

I. Cnidocysts

1. Cnidocyst Biology

The most iconic feature of the cnidarians, and the one for which they are named, are the presence of cnidocysts. These cnidocysts are the vector for the cnidarian venom and the key to their success, as the organelle has not been found in any other phylum yet discovered. As far as structure goes, cnidarians are radially symmetrical in both of their two forms, the mobile medusa form which resembles the classic jellyfish dome, and the sessile polyps which resemble the classic anemone anchored tentacle mass. Reproduction involves the polyps differentiating to produce strobilla and producing disc-shaped ephyra which break off and become medusae (Jouiaei et al., 2015). While this strobilation process in the polyp stage is asexual, cnidarians at the medusa stage undergo either internal or external fertilization depending on the species. One species, *Turritopsis dohrnii*, can even transition between these two forms freely, which allows for both augmented regeneration following injury or stress, and the rejuvenation of the specimen (Piraino et al., 1996). While switching between these forms rearranges their dimensions, the two layers of cells remain distinctly exterior and interior. Cnidocysts are only found in the ectoderm layer in all but the hydrozoa, as they do not aid in digestion. Due to the incredibly small size of many species, the vastness of the biome they dwell in, and the fragility of the species, many aspects of cnidaria are unknown and most research is currently focused on the larger, more common species. As a result, most cnidotoxins known are found in jellyfish and sea anemones.

While the toxins themselves are quite potent, other organisms also contain various toxins that parallel those of the cnidarians. The cnidocyst however, is a unique and highly specialized organelle found only in cnidarians. Even then, most of them concentrate their cnidocysts in the tentacle structures that either hang down from the medusa or project outward from the oral cavity

in the polyp. While there are actually three different subtypes of cnidocysts, the nematocysts, spirocysts and ptychocysts, only the nematocyst is found in all species and thus has the most information available (Özbek et al., 2009). The cells that contain these cnidocysts are referred to as cnidocytes, and are linked into the nervous system of the organism. Typically, each cnidocyte contains one cnidocyst. The cell excretes proteins into a vesicle in its Golgi apparatus where the capsule forms. They can be different dimensions, but they all consist of a series of proteins strands that encapsulate the filament and barb proteins within. The barb faces to the front of the capsule, tethered to the rear of the cnidocyst by a tubular filament (Özbek et al., 2009). The direction of the cnidocyst is easily identified by the cnidocil that projects from the front just off the center, which acts as a trigger to discharge the barb. The capsule itself is comprised primarily of minicollagens, making it exceptionally tough and, therefore, unlikely to leak its venom into the cnidocytes. The barb is capable of easily penetrating lipid bilayers, allowing the filament tube to project the venom into the host cells. The capsules have been found to withstand intense pressures up to 150 bar (Özbek et al., 2009). This structural integrity is vital, as the acceleration of the barb can reach 5,400,000 G's and hit with an impact of 7.7 GPa, which would tear apart a membrane bound organelle attempting to contain such a force. Due to these forces, it is unlikely that the cnidocyst developed as a microscopic defense mechanism, as bacteria would likely be too plentiful to justify the high energy cost of the cnidocyst expenditure. There are many shapes and sizes of cnidocysts, which are positioned recessed into the cell membrane. As the barb leaves the cell, a channel is formed to prevent the creation of a pore and destabilization the cell (Fautin, 2009). Interestingly, there isn't much correlation with cnidocyst morphology and contents, meaning that the toxicity cannot be determined from the capsule alone. It is unclear whether this is due to local environmental influence or irregularity in the individual design of cnidocysts, as it has been found that even members of the same species do not always have the same cnidocyst morphology (Fautin, 2009). A possible explanation lies with the idea that these organelles' evolution is driven by the presence of prey and predators, meaning that exterior forces push the cnidocyst development more so than

its genome, or that there is some phenotypic plasticity when it comes to their specific shape. The toxins themselves are more or less set per species based on its genome, rather than external factors, so the delivery mechanism may be the only shifting point allowing the cnidarian to adapt to the changing ecology around it.

2. Cnidocyst Function

The actual function of the cnidocyst is just as impressive as its structure. The cnidocil extends beyond the interior of the cnidocytes membrane, feeling for the signal to discharge the payload. The signal itself can be an electrical impulse from the nerve network, a chemical signal from the proximity of the prey or even physical contact from another cell's membrane (Anderson and Bouchard, 2009). Once a signal has been received by the cnidocyte, a hinged cover opens at the apex of the cnidocyst called the operculum, out of which the barb is projected at extreme speeds with the filament tubule remaining in contact with the cnidocyte. Upon puncturing the target, the barb inverts and pulls the filament through the hole and into the target cell entirely, during which the cnidocyst itself has fused to its own cell membrane to prevent exchange of cytosol between the two. As soon as the filament is inside the target cell, it begins to release its venom. Overall, the process is still mechanically mysterious, as the entire process is over in nanoseconds, and the different signals most likely work in tandem during that time (Oppegard et al., 2009). Several theories have emerged on the topic of this rapid expulsion, with the most popular being a high pressure differential between the cnidocyst and the exterior environment. This remains plausible, as evidence has shown that calcium ions are built up in the cnidocyst that, when exposed to sea water by the pore formed by the barb, rapidly diffuse out into the media and generate an intense osmotic pressure that pushes the barb and filament out of the capsule (Oppegard et al., 2009). Another theory states that the filament is bound to the minicollagens in the capsule and when they dissociate from the capsule wall, the resulting repulsion of like charged amino acids forces the barb and filament out into the target, but the forces generated are insufficient to account for the observed

projection speed. Interestingly, the cells themselves, being comprised almost entirely of the cnidocyst, are incapable of repairing the cnidocyst after its discharge (Anderson and Bouchard, 2009). The fact that such immense energy expenditure goes into the production of these cnidocyte cells, which are single use, means that the allowance for failed discharges must be very low. prevailing proposed theory involves companion sensory cells that offer supplemental data for discharge signals, and possibly coordinating electrical, mechanical and chemical signals, in order to prevent firing into a non-predator or a prey that is likely to escape the cnidarian (Kass-Simon and Scappaticci, 2002). That said, purified cnidocysts have been induced to discharge using a combination of water and physical stimulation, but this also requires the cnidocysts to be dried prior to the test (Oppegard et al., 2009).

While the true mechanism of the cnidocyst triggering is still unknown; once elucidated, the cnidocyst may present a valuable medical tool. In a sense, the cnidocyst is a microscopic drug delivery system, able to very rapidly disseminate compounds into a specific area. To this end, it could be used to deliver beneficial compounds to specific cells in a patient, like the worlds tiniest syringe. In order for this to be viable, four things must be possible. First, the cnidocysts must be extractable intact, which due to their highly durable nature, does not present a considerable challenge. Next, they will need to be oriented the correct direction, as their cells normally point them towards the exterior and without them, they are unguided. Conjugated lectins were found to anchor the cnidocysts to a surface, but they did not orient them, which poses a challenge to using the cnidocysts *in vivo* (Oppegard et al., 2009). The next hurdle is controlling the discharge, which has been done using water and physical contact, both of which are applicable to nearly all patients. However, the largest stumbling block is that the venom needs to be replaced with the desired chemical without denaturing the capsule. This is a roadblock, as the cnidocysts are both created with the toxin already contained within and cannot be used again after discharging their venom.

Once these challenges are defeated however, the cnidocyst may become a viable micro-applicator for drugs.

II. Cnidarian Toxins

1. Anthozoan Toxins

While the cnidocyst itself is a marvel of molecular design, the venoms contained within are no less impressive for their variability and potency. Sea anemones, sessile cnidarians that are found on coral reefs and other marine waters, possess a diverse range of toxins honed to debilitate organisms unlucky enough to encounter their tentacles. While anemones also use several forms of molecular toxins, the more interesting and varied ones are protein based. There are three main classes of these venoms: enzymes, cytolytins and neurotoxins, of which, the latter is most widely used by anemones (Jouieai et al., 2015). For the enzymatic class, anemones have both Phospholipase A2 (PLA2) and Metalloproteases, the former of which is a highly potent catalyst of the lipids that make up cell bilayers. PLA2's bind to nerve cell membranes and hydrolyze the lipids in order to make them impermeable to neurotransmitters, causing the failure of the synapse (Frazao et al., 2012). The desired effect is generally to paralyze the prey for capture and ingestion. These proteins are small and not used exclusively for venom, rather, they are present in cells of the gut and are used as digestive enzymes as well. The metalloproteases on the other hand, target the extracellular matrix, degrading it and causing local tissue damage (Jouieai et al., 2015). This generally manifests as blisters and inflammation in humans, and is one of the most readily recognizable results of envenomation by cnidarians, aside from local pain. Unlike the other enzymatic toxins, these are used primarily for defense, as the tissue damage is not immediately incapacitating and the prey would likely have withdrawn from the anemone's grasp before the damage became too severe. The next class of toxins, the cytolytins, is pore-forming proteins that provide openings in the membrane to destabilize the homeostasis of the target cell. The largest subsection of these is referred to as actinoporins, and they cause severe complications for both the

cardiovascular and respiratory systems of the unfortunate target (Jouieai et al., 2015). These proteins contain a highly conserved amphiphilic alpha helix at the N terminus, which punctures the cell membrane, a tryptophan heavy segment for binding to erythrocytes, and a repeating Arg-Gly-Asp (RGD) sequence that provides affinity to particular membranes (Frazao et al., 2012). These features allow the protein to effectively bind together on a target cell membrane, and by linking their N termini together, create a pore in the membrane with the alpha helices. This requires a particular surface tag molecule recognition, where most of the specificity of the protein is likely found. Once bound, the helix is extended parallel to the membrane until other like proteins bind and do the same. Once several actinoporins have bound, numerous helices penetrate the membrane, which disrupt the lipid layers and create a small gap between the helices large enough for ions to escape from the cell (Frazao et al., 2012). The loss of these ions triggers a failure of any gradient dependent reaction, and since many actinoporins target the red blood cells, can result in hypotension and cardiovascular failure (Suput, 2009). However, the widest and most signature classes of venom found in anemones are the neurotoxins. As one might expect from a sessile creature unable to give chase, their venom has evolved to be both fast acting and debilitating. The perfect toxin then, is one that causes the target to become even less mobile than the anemone and reduces its resistance to ingestion. To this end, many inhibitor venoms are present in anthozoa, including both sodium and potassium channel inhibitors. The voltage-gated sodium channel toxins (NaTxS) are very small (3-8 kDa as compared to the 20 kDa actinoporins, Jouieai et al., 2015). Furthermore, while they have multiple subunits, they do not form oligomers and can act faster and with a much smaller dosage. The NaTxS bind to sodium voltage channels using their highly conserved alpha domain, stopping sodium ion exchange from the cell, which usually results in cell death (Jouieai et al., 2015). Similar to the sodium channel, the potassium channel has a analogous toxin which is nearly identical in structure and function, but binds to potassium channels rather than sodium channels. However, type II potassium toxins don't bind to channels, rather, they instead bind to proteases and inhibit their ability to degrade trypsin and chymotrypsin and protect

the other venom proteins released in the same cocktail (Jouieai et al., 2015). Interestingly, the type III potassium toxins are capable of binding to both sodium and potassium channels, likely due to their sequence similarly to the NaTx, indicating that they may have a common proteomic ancestor. In contrast to the vast majority of the toxins above, the TRPV1 inhibitor venoms rely on the mammalian response to an errant signal to its pain pathway, triggering an inflammation response without the associated damage to the tissue (Jouieai et al., 2015) These proteins are not well understood yet, but three have been isolated so far: τ -SHTX-Hcr2c, b, and d. These may have potential use as analgesics if they can be replicated more easily. Unfortunately, anthozoa cnidocysts contain a great variety of venom proteins which make isolating any particular one difficult to perform en masse.

2. Medusozoan Toxins

Medusozoa, on the other hand, are far more widespread and due to their medusa stage, can be numerous within the same body of water. Like the anemone, the jellyfish has a polyp stage where they are sessile, but they are generally more recognizable in their larger, medusa stage of development. While mobile, they are still by no means agile, stalking predators and still rely heavily on their venom for both hunting and defense. One particular class, the cubozoa, have caused over 50 human deaths from their stings, and considering their miniscule size, their venom is considered one of the world's most potent (Tibballs, 2006). The cnidocysts of the *Chironex fleckeri* (box jellyfish) are not particularly extraordinary, nor are all cubozoa as potent killers as the box jellyfish. Mice injected with 35,000 cnidocysts worth of venom died within 2 minutes, with loss of extremity control progressing up to cessation of breathing and finally cardiac arrest. Suffice it to say, the venom is exceptionally dangerous, and as such, research has been slow and careful. The overall venom shows hemolytic and necrotic tendencies; and the hemolysin protein has been isolated, but failed to perform under clinical test (Tibballs, 2006). Flushing the point of envenomation with vinegar has been proven to inhibit the venom, as does blocking the calcium channel in the affected

cells, but the mechanism of the latter is still undetermined. A related venom in other cubozoa, CrTX, has been found to open up calcium channels indefinitely, particularly in smooth muscle and intestinal lining (Tibballs, 2006). This protein causes the muscles to continuously contract, eventually stressing them to the point of death, but it can be removed with calcium channel inhibitors or antagonists. Unlike many of the previous venoms, CrTX is also quite large, 46 kDa, and is closely related to other cubozoan venoms (Tibballs, 2006). The other major class of jellyfish, scyphozoan, are globally distributed from tropic to arctic oceans. These jellies are generally larger and their venom is more easily extracted. A particularly common species, the moon jellyfish (*Aurelia aurita*), is found throughout all of the non-Artic or Antarctic oceans and is generally found to be harmless to humans (Mariottini and Pane, 2010). The venom found in its cnidocysts consists of several mild proteotoxins. One is a weak proteolytic enzyme, which causes muscle twitches and has been shown to irreversibly depolarize the muscle membrane, which is associated with an increase of sodium ion flow through the membrane, a likely indicator that it may be a NaTX (Jouieai et al., 2015). Another venom extract exhibited phospholipase A2 activity and, much like the anemone enzyme, causes nerve blocking in the target. All in all, the effect to most human cases is little more than an itch and some skin irritation, as the venom is either very dilute or lacking potency (Mariottini and Pane, 2014). While this cnidarian is mostly a nuisance in the Mediterranean, other examples of the moon jellyfish in the Caribbean have had near lethal levels of these proteins extracted from their tentacles, including hemolytic proteins similar to those found in anemones. Another species, the mauve stinger (*Pelagia noctiluca*), also exhibits these dermatotoxic venoms and while it can regenerate its stinging battery rapidly, the cnidocysts simply do not penetrate deep enough into the human skin to reach greater vessels where its hemolytic venom would be a danger (Mariottini and Pane, 2010). Overall, jellyfish medusa possess a greater threat to humans simply due to contact in open water, as corals and anemone are stationary and benthic, therefore encounters are rare. Treatment of envenomation generally involves introduction of a mild acid, like acetic acid (aka vinegar), and keeping the affected region clear of physical irritation which may cause more

cnidoblasts to discharge (Cegolon et al., 2013). Despite the danger presented by these cnidarians, research continues to demystify their venom and determine possible remedies, uses, and treatments.

III. Hyaluronidase in *Chrysaora quinquecirrha*

The sea nettle, *Chrysaora quinquecirrha*, (also known as the Atlantic or Stinging Sea Nettle) is a particularly common cnidarian along the Mid-Atlantic coast of the United States (Mariottini and Pane, 2010). As a typical scyphozoan, they have a sexual medusa life history stage and an asexual polyp stage, both of which possess stinging nematocysts housing a cocktail of venoms (Long-Rowe and Burnett, 1993). While it's able to hunt a wide variety of organisms (Meredith et al., 2016), its venom is more of a nuisance than a threat to humans; with stings causing pain and irritation, but not incapacitation. One such protein in its venomous arsenal is hyaluronidase, which is not a true venom. Hyaluronidase hydrolyzes the glycosaminic bonds in hyaluronic acid found throughout the extracellular matrix in epithelial and connective tissue layers. Hyaluronic acid is one of several glycosaminoglycan polymers that form the bulk of the extra cellular matrix, and breaking these polymers causes the matrix to become more fluid and allows for other venom proteins to spread more easily and widely throughout the target's tissues, affecting a greater number of cells and increasing the potency of the overall envenomation. Hyaluronic acid is synthesized in the plasma membrane of vertebrate cells, where low molecular weight polymers of hyaluronic acid suppress its production (Smith and Ghosh, 1987). Despite this, there is generally enough other glycosaminoglycan polymers to prevent the total breakdown of the matrix. Since its target molecule is a key component in extracellular matrixes throughout the animal kingdom, hyaluronidase is utilized by an equally wide range of organisms as a co-venom. Many creatures from cnidarians to hornets and rattlesnakes use hyaluronidase in their venom suite, which remains largely conserved despite the wide phylogenetic differences among them. Not all jellyfish have been found to possess hyaluronidase, with recent tests showing that among four jellies tested: Flame Jelly (*Rhopilema escukenta*), Nomura's jelly (*Nemopilema nomurai*), Ghost jelly (*Cyanea nozakii*)

and Moon Jelly (*Aurelia aurita*); only Flame jellies exhibited hyaluronidase activity (Lee et al., 2011). Since the target bond is specific and conserved, the enzyme maintains its overall structure and thus its sequence to some degree in order to maintain activity.

IV. Hyaluronidase in other animals

Hyaluronidase is a widespread co-venom, utilized from cnidarians up to chordates. Hyaluronic acid is a key component of the chordate extracellular matrix, which hyaluronidase is designed to break down. Mammalian hyaluronidase can break down the polymers, which can be millions of daltons in weight, into tetramer units (Chao et al., 2007). Similarly, stonefish (*Synanceja horrida*) venom hyaluronidase was found to break down the polymers into tetramers, hexamers, octamers and decamers with fewer large polymers (Sugahara et al., 1992), which may indicate a size limitation in binding to the enzyme. These low molecular weight hyaluronic acid polymers induce an inflammatory response in the host, which causes the host to clear out damaged or dead cells, allowing even greater spread of the venom (Kemperaju and Girish, 2006; Fox, 2013). The activity of Indian Cobra (*Naja naja*) venom hyaluronidase was found to be inhibited by the presence of heparin sulfate and dermatan sulfate, which are also found in the extracellular matrix (Girish and Kemparaju, 2005) and may partially or incorrectly bind to hyaluronidase. Honey bees (*Apis mellifera*) also use hyaluronidase, which has been fully sequenced and crystalized (Markovic-Housley et al., 2000). Despite its relative taxonomic distance from humans, bee hyaluronidase shares its primary and all of its secondary sites with all human hyaluronidases, and features thirty percent sequence homology. Most of the conservation occurs in the active site groove, with greater variety amongst the outer parts of the protein (Markovic-Housley et al., 2000). Hyaluronidase is also used in mammalian sperm to break down the protective shell of hyaluronic acid surrounding the ova, where it is anchored into the cellular membrane (Gacesa et al., 1994). Even with its eventual purpose changed, the activity of the enzyme remains unchanged, so even here the conservation is similar despite the membrane anchor (Gmachl and Kreil, 1993). Since the

hyaluronidase of sea nettles has been detected but not sequenced, the reveal of such a sequence could aid in the discovery of the origin point of hyaluronidase in humans.

V. Specific Aims

To this end, a putative mRNA of *Chrysaora quinquecirrha* hyaluronidase has been produced by transcriptome analysis (Gaynor, Shchegolev, Meredith, Bologna, and Pavan, unpublished) and was used to design primers that can amplify the corresponding genomic region of this gene. From the DNA sequences, homology with the human SPAM1 gene can be compared to see sequence retention. Since the venom protein will lack a membrane anchor and could possess a destination tag for the cnidocyst, the difference in sequence at these sites will likely be quite high and could help identify such a tag. Furthermore, the extraction of hyaluronidase from the cnidocysts will allow for comparative testing of activity between it and other hyaluronidase enzymes. The purified hyaluronidase would also provide a conformation that the gene sequenced was in fact venom hyaluronidase and not a hitherto unknown digestive enzyme. Since much of the sea nettle's genome is still unsequenced, the hyaluronidase sequence discovered in this research, especially if it was proven to be a component of the sea nettle venom, could prove useful in determining the signal peptide and propeptide sequences required for cnidocyst import. The overall aim of this research is to clarify this hypothesis and provide a definitive sequence and activity for *Chrysaora quinquecirrha* venom hyaluronidase.

Materials and Methods

I. *Chrysaora quinquecirrha* Transcriptome by RNA-Seq Analysis

1. Isolation of Total RNA from *Chrysaora quinquecirrha*.

Total RNA was isolated from the tentacles of a single medusa collected from the Catus Island region of Barnegat Bay (collected August 10, 2013). This individual was transported back to the laboratory and washed several times in sterile artificial seawater (19 ppt). It was kept alive for 2 days to allow time for all gut contents to be expelled. It was then rinsed again with artificial seawater to remove any other (non-jellyfish) DNA/RNA. Tentacles were frozen in liquid nitrogen and ground to a fine powder with a homogenizer. Total RNA was isolated using the Qiagen RNeasy Plus MicroKit (Cat No./ID: 74034) following the manufacturer's instructions.

2. Preparation of NGS Library. Library preparation was performed by GeneWiz, Inc. (South Plainfield, NJ) and included separating out poly A+ RNA (to eliminate or minimize the inclusion of rRNA and tRNA), construction of a cDNA (complementary DNA) library by reverse transcription, and shearing of cDNAs to produce fragments ranging from 100 to 200 bp in length. Ends of dsDNA were repaired and adaptors ligated to ends to permit multiplexing of samples.

3. NGS Sequencing. DNA was sequenced on an Illumina HiSeq 2500 platform using 2 x 100 paired ends. Approximately 380,000,000 reads were generated from this run from triplicate samples.

4. Contig Assembly. Raw sequence data were processed by eliminating sequences with low quality scores, removal of adaptor sequences, and then assembling using CLC Workbench to generate a file of 87,600 contigs (JG01-CQTTtotalRNA-Contigs.fasta). The data were

organized as a series of fasta files, with the first line indicating the contig number and the approximate coverage of the assembled sequence.

5. BLAST Search. This file of assembled contigs was BLASTed against the nr database of Genbank (this is the complete Genbank collection of all known sequences) and the best hit (highest score match or lowest E or Expect value) was recorded in a second file (rna.nr.best.hit.complete.xlsx). Subsequently, these BLAST hits were cross-indexed to the UniProt Venom Database (<http://www.uniprot.org/program/Toxins>).

II. DNA Isolation from *Chrysaora quinquecirrha*

1. CTAB/NaCl Method

This procedure was adapted from Winnepeninckx et al. (1993) and was performed as follows: two hundred mg of CTAB (cetyltrimethylammonium bromide) and 5.78 ml of sterile deionized water were transferred to a sterile 15 ml plastic tube and swirled under hot water until fully dissolved. Next, 1 ml of 1 M Tris buffer (pH 8.0), 2.80 ml of 5 M NaCl, 400 μ l of 0.5 M EDTA, and 20 μ l of β -mercaptoethanol were added in order to the tube, having been transferred to a sterile chemical hood prior to the addition of the β -mercaptoethanol. 1 mg of proteinase K was then added and the tube capped and gently inverted to fully mix the solution. While under the same chemical hood, two *Chrysaora quinquecirrha* samples previously collected from the Toms River (J. Gaynor) and stored in ethanol were decanted and transferred to a sterile 15 ml tube. The two tubes were centrifuged for 5 minutes at 3000 rpm and decanted again, then transferred to a petri dish. There, each specimen was briefly allowed to evaporate, then severed into four roughly equal pieces using aseptic scalpels. These pieces were transferred to sterile 1.5 ml Eppendorf tubes. To these tubes, 500 μ l of the CTAB solution was transferred and the samples ground for 1 min with a sterile micropestle. The tubes were then incubated at 60°C for one hour, inverting the tubes occasionally. After incubation, 0.5 ml of chloroform:isoamyl alcohol (24:1) was added to each tube, inverting gently for 2 minutes to mix. Then the tubes were spun at 14,000g in a microcentrifuge at 4°C for 10 minutes. Carefully, the upper aqueous phase of each tube was transferred to a new sterile 1.5 ml tube without introducing the solid material at the interface to the new tube. Then two thirds the total volume of each sample of isopropanol was added. The tubes were inverted several times and stored overnight in 4°C. These tubes were then spun at 14,000g in a microcentrifuge at 4°C for 15 minutes. The supernatant was carefully removed and replaced with 500 μ l of 70% ethanol and spun at 14,000g in a microcentrifuge at 4°C for 15 minutes. This step was repeated, removing the supernatant after the third spin. Samples were dried in a Savant Speed-Vac for two cycles of 5

minute spins without heat, after which the dried pellets were resuspended in 40 μ l of TE (10 mM Tris, pH 8.0; 1 mM EDTA), adding half the total amount at a time. The tubes were stored overnight in -20°C , then thawed and consolidated into two tubes, TR1 and TR2 containing the entirety of each jellyfish extract respectively.

2. Chelex 100 Method

Alternatively, DNA was extracted using a rapid method that relied on boiling of soft samples in the chelating agent Chelex 100 (Bio-Rad). Samples were transferred into a sterile 1.5 ml Eppendorf tube containing 300 μ l sterile 5% (w/v) Chelex 100 in 50 mM Tris base pH 11, ensuring the source was smoothly agitated to evenly distribute the Chelex beads. Tubes were kept on ice, vortexed for several seconds to mix, then heated at 100°C in a dry heat block for 10 minutes, keeping the tubes closed throughout the process. Tubes were then transferred to an ice bath for 2 minutes, vortexed again for several seconds, then centrifuged at 16,000g for 10 minutes at 4°C . Finally, 50 μ l of the supernatant was transferred to a new sterile 1.5 ml tube and stored at -20°C until use. Two μ l was removed for NanoDrop analysis.

3. RNase Treatment

DNA samples were subjected to an RNase A treatment to prevent carryover of RNA contamination in DNA preparations. To ensure that the RNase A preparation (Aldrich-Sigma, Cat R1149) was free of contaminating DNase activity, I prepared identical *Chrysaora quinquecirrha* DNA samples that were both treated and untreated with RNase A. Two- μ l samples of TR1 and TR2 (2.2 And 2.0 μ g DNA total, respectively), with and without 1 μ l of RNase A (10 mg/mL), along with negative controls of water and water with RNase A were separated on a 1% (w/v) agarose gel. RNase A treatment of the DNA samples was at 37°C for 30 minutes prior to loading on the gel. Samples were electrophoresed for 45 minutes at 100 Volts (Figure 1). The gel contained SYBR-Safe (1X; Invitrogen) which was excited by blue light (477 nm) allowing for a Kodak

ImageStation 440CF to capture the image. From the test gel (Figure 1), neither appreciable loss in DNA quantity, nor introduction of new particles is observed from treatment of RNase A.



Figure 1. Estimation of gDNA (genomic DNA) size and integrity and test of DNase contamination of RNase A preparation. Lane 1 & 10, 10 μ L of Hi Lo DNA Ladder (Minnesota Molecular, Inc., www.mnmolecular.com); Lane 2, 10 μ L of DNA from TR1 amplified with HyalF and HyalF without RNaseA; Lane 3, 10 μ L of DNA from TR1 amplified with HyalF and HyalF with RNaseA; Lane 4, 10 μ L of DNA from TR2 amplified with HyalF and HyalF without RNaseA; Lane 5, 10 μ L of DNA from TR2 amplified with HyalF and HyalF with RNaseA; Lane 6, 10 μ L of Negative control with RNase A; Lane 7, 10 μ L of Negative control without RNase A; Lane 8 & 9, empty.

III. Primer Design

Primers were designed using the PrimerQuest (<http://www.idtdna.com/Primerquest/Home/Index>) and OligoAnalyzer (<http://www.idtdna.com/calc/analyzer>) tools available online from Integrated DNA Technologies (Table 1). Generally speaking, primers designed for this project were between 17 and 30 base pairs in length, had a T_m (melting temperature) of between 60 to 65 °C, and both members of a primer pair had a T_m within 5°C of each other to ensure both bind with similar kinetics.

IV. PCR Amplification

PCR amplifications were performed using ChoiceTaq Master Mix (Denville Scientific, Denville, New Jersey, USA) according to manufacturer's directions with the exception that I used 20 μ L reaction volumes. Primers used for amplification of the hyaluronidase gene are listed in Table 1. PCR was carried out in a ProFlex Thermal Cycler (Applied Biosystems, Inc.) according to the following parameters: 95 °C for 1 min (1 \times); 95 °C for 30 s, 55 °C for 30 s, and 72 °C for 90 s (30 \times); 72 °C for 7 min (1 \times); followed by a hold at 4 °C. Positive and negative template controls were typically run and 10 μ L of each sample was run on a 1% (w/v) agarose gel to assess purity and yield of PCR product.

Table 1. List of primers used on TR1 and TR2

Primer Name	Regional Area on the RNASeq	Sequence
HyalF	3' tailing region	CGGATCCATAGCACGTTTCT
HyalR	5' central region	ATAATGGCCTCCAAGGTTCC
HyF	3' end of HyalF amplicon	AGCCTCGTATTTACGTACC
HyR	5' end of HyalR amplicon	GCACTGCATTATTTCCATCGT

V. DNA Sequencing and Bioinformatic Analysis

PCR products were subject to direct Sanger dideoxy sequencing on an ABI3130 Genetic Analyzer. Sequencing reactions were carried out using BigDye Terminator Ready Reaction Mix V3.1 according to manufacturer's instructions except that I used 1/16 diluted reactions. Excess unincorporated fluorescent dideoxy nucleotides were removed by Performa Gel DTR Gel Filtration Cartridges (EdgeBio, Gaithersburg, Maryland, USA). Both strands of each product were sequenced using the same primers used to generate the fragment. Raw sequences were initially edited and aligned using 4 Peaks from Nucleobytes (<http://nucleobytes.com/4peaks/index.html>) and CLUSTAL Omega (Sievers et al., 2011; <http://www.ebi.ac.uk/Tools/msa/clustalo/>), and searched for homology against all known genetic sequences using the BLAST algorithm (Altschul et al., 1990). Additionally, alignments and assembly of contigs was accomplished using Geneious R10 (www.geneious.com) bioinformatic software. Individual electropherograms were proofread and edited for accuracy manually, and consensus sequences were derived from overlapping segments. Unclear segments or low quality sequence data were omitted. Raw and edited gDNA sequences of the hyaluronidase gene were initially mapped to the partial mRNA sequence of this gene found in our RNA-Seq library. This method permitted the discovery and mapping of introns in gDNA since any introns present in the gDNA would have been spliced out and removed from mature mRNA used to generate the RNA-Seq library. Many sequences generated from both TR1 and TR2 gDNA samples together create a more confident sequence of these introns as well as their intron/exon junctions.

VI. Hyaluronidase Assay

To determine the activity or presence of hyaluronidase in *Chrysaora quinquecirrha*, a standard turbidimetric assay was performed (Dorfman, 1955) with modifications to accommodate smaller sample volumes. Standard hyaluronic acid (0.03% w/v in 300mM sodium phosphate, pH 5.35 at 37°C) was used as a substrate and purified bovine testicular hyaluronic acid (0.025 mg/ml in 20

mM Sodium Phosphate, pH 7.0 at 37 C with 77 mM Sodium Chloride and 0.01% Bovine Serum Albumin) was used as the reference standard, both obtained from Sigma Aldrich. The enzymatic samples were obtained from Dr. Gaynor from previously collected and isolated cnidocysts. These purified cnidocysts (PN 8/07/14) were sonicated in 1 minute segments (6 times), allowing samples to cool on ice for 90 seconds in between each sonication period. The tube containing the sample and the sonicator probe tip were also sealed with Parafilm to prevent sample loss, and following the sonication, the sample was centrifuged (5 minutes at 6,000 x g) and the supernatant transferred to a sterile 1.5 ml Eppendorf tube. A series of sterile 1.5 ml tubes were labeled as detailed in Table 2, and incubated at 37°C for 10 minutes.

Table 2. Standard Layout for Hyaluronidase Assay. All values represent mL; final volume in all tubes was 0.25 mL. E represents Enzymatic sample, S represents Standard sample.

	Blank	E1	E2	E3	S1	S2	S3	S4	S5
Enzyme	0	0.025	0.05	0.075	0	0	0	0	0
Standard	0	0	0	0	0.005	0.025	0.05	0.075	0.1
Dilutant	0.25	0.225	0.2	0.175	0.245	0.225	0.2	0.175	0.15

Following the incubation, 0.25 ml of the substrate solution were added to each tube and they were set to incubate for another 45 minutes, after which, 0.25 ml of each tube was transferred to a clean cuvette containing 1.25 ml of acid albumin solution (24 mM Sodium Acetate with 79 mM Acetic Acid and 0.1% Bovine Serum Albumin pH 3.75 at 37 C containing 1:1 HCl:H₂O) and allowed to rest for 10 minutes at room temperature. The fluid was circulated gently to prevent settling without creating bubbles, then placed into a spectrophotometer at 600 nm and blanked with deionized water. The A_{600nm} values were recorded and set to a standard curve to compare the activity

of the cnidocyst hyaluronidase. The standard hyaluronidase is known to have 10 units/ml at the concentration prescribed, where 1 unit is defined as a U.S.P. National Formulary Unit effecting turbidity. From this curve and the enzymatic sample curve, the activity respective to the standard was formulated.

Since hyaluronic acid is clear at low concentrations, visual observation of its concentration is difficult and inaccurate. Instead, sodium acetate is used to act as an indicator for the amount of hyaluronic acid preserved in an active state, by allowing the hyaluronic acid to catalyze the dissolution of sodium acetate and cause the opalescence of the solution to increase. The opalescence can be visually and spectrophotometrically qualified, and the relationship between the concentration of hyaluronic acid and this reaction is linear. Using bovine testicular hyaluronidase as a standard, a concentration curve was formulated first (Figure 2), along with a kinetics reaction curve at a concentration of 60% (Figure 3). Both curves followed a logarithmic pattern likely as a result of enzyme saturation. A low concentration standard curve was formulated second along with the *Chrysaora quinquecirrha* cnidocyst enzymatic curve (Figure 22). This curve followed a more linear relationship, as is expected of single stage enzymatic activity.

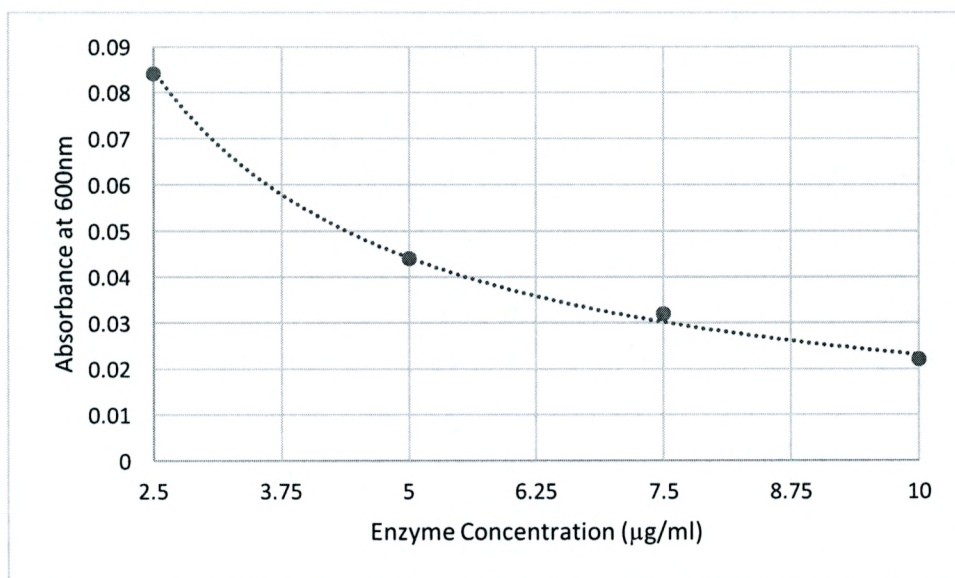


Figure 2. High concentration standard curve of bovine testicular hyaluronidase incubated for 45 minutes. All samples were blanked with and equal volume of deionized water prior to measurement. The control absorbance (0.512) was left out for legibility of the graph.

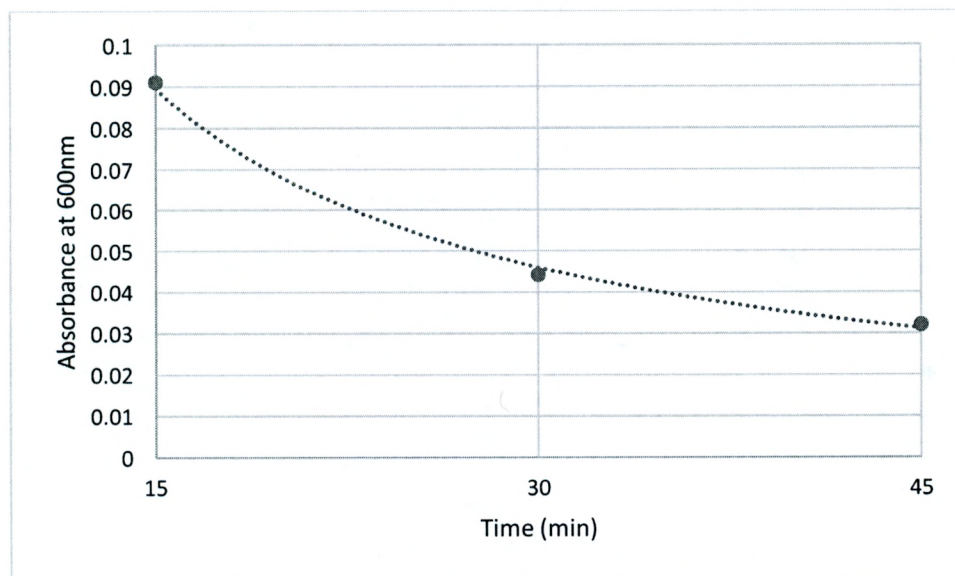


Figure 3. Bovine testicular hyaluronidase standard curve for 7.5 µg/ml over time. All samples were blanked with and equal volume of Di water prior to measurement. The control absorbance (0.512) was left out for legibility of the graph.

Results

I. Evidence for Hyaluronidase Expression in the *Chrysaora quinquecirrha* Transcriptome

Previous research (Gaynor, Meredith, Shchegolev, and Bologna, unpublished) has generated a transcriptome from tentacles of a *Chrysaora quinquecirrha* medusa. Sequencing of the RNA-Seq library generated over 3,800,000 reads which were assembled into 87,600 unique contigs (Meredith & Pavan, unpublished). A comprehensive search of individual contigs against the NCBI database using the BLASTX algorithm (Altschul et al., 1997) has identified 30,817 hits with Expect (E) value of 10^{-4} or less. A search of this list of proteins found one match (Contig 20047; Figure 4) of 925 bp showing significant homology to hyaluronidase proteins found in many animals including two Cnidarians, *Hydra vulgaris* and *Acropora digitifera* (Figure 5). With the two cnidarians, the identical amino acid matches were at 56% and 51%, but drop to 43% with the more distantly related species. However, the query coverage is high, indicating a widely distributed matchup across the contig. In further analysis, the matchup with *Hydra vulgaris* hyaluronidase protein indicated that the *Chrysaora quinquecirrha* contig was not long enough to match the entirety of the *Hydra vulgaris* sequence, but matched at nearly its entire length, suggesting that this contig was only a partial sequence for *Chrysaora quinquecirrha* hyaluronidase (Figure 6). The hyaluronidase from *Acropora digitifera* was even longer, indicating that larger hyaluronidases do exist and the identified sequence from *Chrysaora quinquecirrha* could be larger. However, *Hydra vulgaris* is less removed from *Chrysaora quinquecirrha* than *Acropora digitifera*, coinciding with the higher homology between these two hyaluronidases.

>JG01- *Chrysaora quinquecirrha*

TotalRNA_GAGTGG_L003_R1_001_filtered_(paired)_contig_20047 Average coverage: 24.29
TTAAATCACTGCTTAGATGGGCCTTGCGAACACAGCGACCGGATCCATAGCACGTTT
CTCTGCTACATTTTTCAACCTCGCTTCGGATATGACTAATTGATGGTCCAAGAGTGCT
TTGAATGTATGTGTTGATTCTATGGCAAACATCAGGTGACGTGTTTTTCATCATTCTG
TTGCCCCAAATGACTACGCCAGCTGCACCCATTTTCAGAGGCAACGCCAATAGTGTTA
TAAAGATCATTCCGATCAAGAAAATTGAACTGTAAAGGATGATCCATATAAATACTT
CTGAAATATGGAAATAAGGGAAGAACATCTTTGCCATGACGCTGTGATAAACGAAG
AGTGACACGAAATGCTTCTCGTAATCTTCCTTTGACATAATCAGGGTTCTCTAAGTGG
CTTTTTAGTAAATATAACGATGGAAATAACGCAGTGCTTTCTGCAAATAGCCAGTCT
ATTTTGTGCTTATTTTCGTTTTACCTTGTCTGTACATTGGAAATCGTATTTTTCTTGCCC
AAAACAATCCGGAAAACCATAAAAACCCCATATGCTTTTGGTCTTAGCCTCTTTCC
CAATCTGATTGTCTCAACGAACATTGAGCGTGCTGCAGCCTCGAATTGATCTTTAGCC
TCTAAAACGAGATCCGTCATTGACCAATCAGGATGATGCTTTCTTACTAAATCAACC
GATTTGATTTTGTAGATTTTCTTAGAATTCCAATTTCTTTCCATAATGGCCTCCAAGG
TTCCAATCAATAACAGCGAGGCCGTTGTAGTGAGGGTCCGGGATTCTTGACATGAT
GTCTTGTTTTGCTCTTACTAAATGATCGTGAAGGTTTACCAGCTGAGGCAGACCGCCG
TTGAAATTAGTTTCTCCATCGTCTGATAAATAATACGGATAAAGACCAAGTTGTGCTC
CATA

Figure 4. Raw sequence read of Contig 20047 generated from *Chrysaora quinquecirrha* transcriptome. Contig contains 925 bp and was assembled with an average coverage of 24.29X.

Sequences producing significant alignments:

Select: All None Selected: 0

Description	Max score	Total score	Query cover	E value	Ident	Accession
<input type="checkbox"/> PREDICTED: hyaluronidase-1-like [Hydra vulgaris]	360	360	91%	4e-120	56%	XP_012557317.1
<input type="checkbox"/> PREDICTED: hyaluronidase-1-like isoform X1 [Acropora digitifera]	345	345	98%	2e-111	51%	XP_015767767.1
<input type="checkbox"/> PREDICTED: hyaluronidase-1-like isoform X2 [Acropora digitifera]	345	345	98%	2e-111	51%	XP_015767768.1
<input type="checkbox"/> PREDICTED: hyaluronidase-1 [Ovis aries]	258	258	97%	5e-80	43%	XP_004018490.1
<input type="checkbox"/> PREDICTED: hyaluronidase-1 [Pantholops hodgsonii]	258	258	97%	7e-80	44%	XP_005969361.1
<input type="checkbox"/> PREDICTED: hyaluronidase-1 [Capra hircus]	258	258	97%	1e-79	43%	XP_005695987.1
<input type="checkbox"/> PREDICTED: hyaluronidase-1 [Monodelphis domestica]	256	256	98%	4e-79	42%	XP_007499963.1
<input type="checkbox"/> PREDICTED: hyaluronidase-1 isoform X1 [Nomascus leucogenus]	254	254	97%	2e-78	43%	XP_003257149.1
<input type="checkbox"/> PREDICTED: hyaluronidase-1 isoform X1 [Pongo abelii]	253	253	97%	3e-78	43%	XP_002813766.3
<input type="checkbox"/> PREDICTED: hyaluronidase-1-like [Lalimeria chalumnae]	253	253	98%	4e-78	42%	XP_005992716.1
<input type="checkbox"/> PREDICTED: hyaluronidase-1 isoform X1 [Chlorocebus sabaeus]	253	253	97%	4e-78	43%	XP_007982497.1
<input type="checkbox"/> hyaluronoglucosaminidase 1 isoform 2 [Homo sapiens]	253	253	97%	5e-78	43%	AAD24460.1
<input type="checkbox"/> PREDICTED: hyaluronidase-1 isoform X2 [Mandrillus leucophaeus]	253	253	97%	6e-78	43%	XP_011848654.1
<input type="checkbox"/> PREDICTED: hyaluronidase-1 isoform X1 [Macaca mulatta]	253	253	97%	7e-78	43%	XP_001102414.2
<input type="checkbox"/> Chain A, Structure Of Human Hyaluronidase 1, A Hyaluronan Hydrolyzing Enzyme Involved In Tumor Growth And Angio	252	252	97%	1e-77	43%	2PE4_A
<input type="checkbox"/> PREDICTED: hyaluronidase-1 isoform X1 [Pan troglodytes]	252	252	97%	1e-77	43%	XP_516477.2
<input type="checkbox"/> hyaluronidase-1 isoform 1 precursor [Homo sapiens]	252	252	97%	1e-77	43%	NP_149349.2
<input type="checkbox"/> hyaluronoglucosaminidase 1 [synthetic construct]	251	251	97%	2e-77	43%	AAX29960.1
<input type="checkbox"/> PREDICTED: hyaluronidase-1 isoform X1 [Colobus angolensis palliatus]	252	252	97%	2e-77	43%	XP_011794407.1
<input type="checkbox"/> PREDICTED: hyaluronidase-1 [Rhinopithecus roxellana]	251	251	97%	2e-77	43%	XP_010367484.1
<input type="checkbox"/> PREDICTED: hyaluronidase-1 [Gekko japonicus]	251	251	97%	2e-77	43%	XP_015273339.1
<input type="checkbox"/> PREDICTED: hyaluronidase-1 [Bubalus bubalis]	252	252	97%	2e-77	43%	XP_006053369.1

Figure 5. BLASTX results of the *Chrysaora quinquecirrha* RNA contig 20047 encoding the venom hyaluronidase gene. Although this is only a partial list of matches, this analysis demonstrates the highest homology is seen to Cnidarians. *Hydra vulgaris*, which matched with an Expect (E) value of 4×10^{-120} , was used as the query going forward due to its phylogenetic distance from *Chrysaora quinquecirrha*.

Alignment of the putative *Chrysaora quinquecirrha* hyaluronidase protein with that from *Hydra vulgaris* showed remarkable homology, with a 56% identity and 79% positive conservation over the 282 amino acid length (Figure 6). The BLASTX algorithm inserted two gaps in the *Hydra vulgaris* sequence to maximize matching to that from *Chrysaora quinquecirrha*.

Score	Expect	Method	Identities	Positives	Gaps	Frame
360 bits(925)	2e-126()	Compositional matrix adjust.	159/282(56%)	225/282(79%)	2/282(0%)	
Features:						
Query	79	AQLGLYPYYVLN-GDKNYNGGLPQLVDMNEHLRKARLDIINRIPDESFNGLAVIDWEPWR				137
Sbjct	3	AQLGLYPYY+ + G+ N+NGGLPQLV++++HL +A+ DI++RIPD +NGLAVIDWEPWR				62
Query	138	PVWETNWKRIYKVRVELVRSKHPHWLTKLIEKAKQDFEEAAKNFFINTINLGKQLR				197
Sbjct	63	P+WE NW +K+IYK++SV+LVR HP W+++ L+ +AK FE AA++ F+ TI LGK+LR				122
Query	198	PKALWGFYGFPCFAHEENHYQCSSEVQKFNDRLDWLFQSSTALFPPSMYLLDEHPDNRDY				257
Sbjct	123	PKALWGFYGFPCF E+ +QC+ +V++ ND++DWLF STALFPS+YLL H +N DY				182
Query	258	VLGRLRETLRFASKGVGKNSRNI-PIFAYHRNIYENNPLAFNFLTAKADLDNTVGLAADIG				316
Sbjct	183	V GRLRE R + ++ +++ P+F Y R+IY ++PL FNFL + DL NT+G+A+++G				242
Query	317	ASGIIVWGNRFDENTSPEVCHKIDTYIATKLGPIYQNKQRQL		358		
Sbjct	243	A+G+++WGNR DENTSP+VCH+I+TYI + LGP I + + ++		284		

Figure 6. Putative hyaluronidase amino-acid sequence from *Chrysaora quinquecirrha* queried against *Hydra vulgaris* hyaluronidase. Note that the RNA-Seq generated sequence is the subject (Sbjct) and *Hydra vulgaris* hyaluronidase is the Query. Plus (+) signs indicate substitution of a conserved amino acid, and dashes (-) indicate positions where gaps were inserted to maximize alignment.

II. Hyaluronidase Gene Structure from *Chrysaora quinquecirrha*

From contig 20047, an initial pair of primers (HyalF and HyalR) were generated, as indicated in Figure 7. The primers were spaced 674 bp apart, allowing for the generation of an amplicon that was a reasonable length for reliable sequencing. However, upon running the PCR reaction and analyzing the amplicons by electrophoresis, both TR1 and TR2 generated sequences of *ca.* 2900 bases in length (Figure 8), considerably larger than expected. Notably, TR2 produced a doublet with bands at both 2900 and 2800 bp. The upper band of this doublet corresponds to the band from TR1; however, the lower band presumably has a size difference which may be due to the absence of an insertion sequence located in the inner intron. Since the bands were far larger than anticipated, additional primers were designed in order to create an overlap between the pairs and allow for

generation of amplicons to assist in the alignment and assembly process. Inner primers (HyF-R) were developed from these sequences which generated sequences *ca.* 1200 bases in length (Figure 8), and a combination of the Hyal and Hy primers generated a sequence *ca.* 2250 bases in length (Figure 8). Sizes of amplicons were estimated from the HiLo DNA ladder accompanying the DNA in the electrophoresis gel, which contains a collection of sized fragments of DNA (Figure 9).

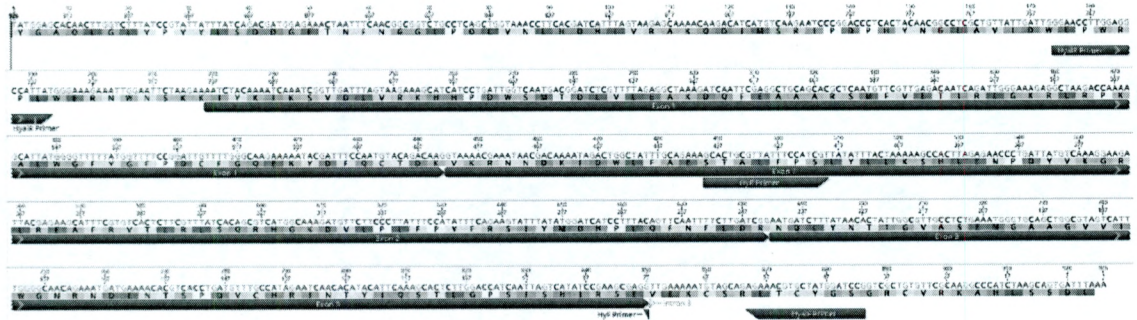


Figure 7. RNA seq with DNA annotations. Primers are indicated in green, pointing in the direction of their 3' ends. Exons are annotated in black, numbered incrementally from 5' to 3'. Intron 3 is indicated with a white placeholder, as introns are not located on the RNA seq.

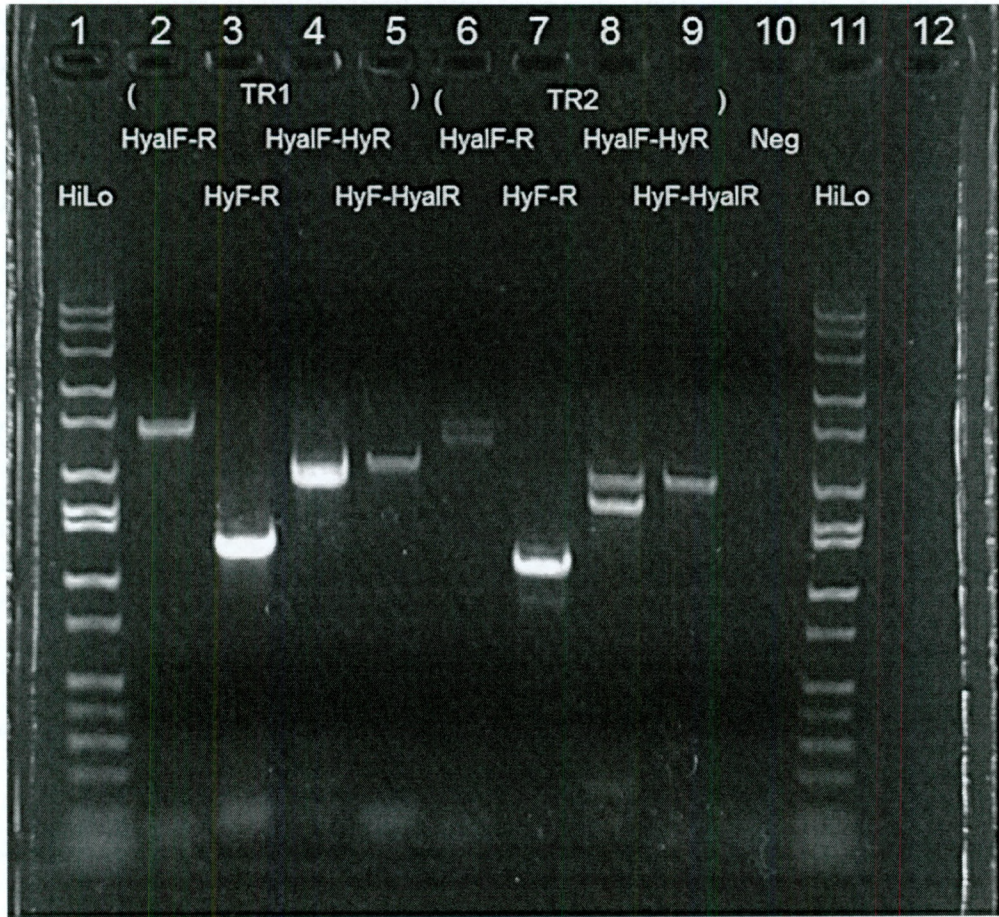


Figure 8. DNA fragment sizes generated by HyalF/R and HyF/R from TR1 and 2. The HiLo DNA ladders are of consistent size, as shown in Figure 5, and used to determine the size of the amplified bands. Lane 1 & 11, 10 μ L of Hi Lo DNA Ladder (Minnesota Molecular, Inc., www.mnmolecular.com); Lane 2, 10 μ L of DNA from TR1 amplified with HyalF and HyalR; Lane 3, 10 μ L of DNA from TR1 amplified with HyF and HyR; Lane 4, 10 μ L of DNA from TR1 amplified with HyalF and HyR; Lane 5, 10 μ L of DNA from TR1 amplified with HyF and HyalR; Lane 6, 10 μ L of DNA from TR2 amplified with HyalF and HyalR; Lane 7, 10 μ L of DNA from TR2 amplified with HyF and HyR; Lane 8, 10 μ L of DNA from TR2 amplified with HyalF and HyR; Lane 9, 10 μ L of DNA from TR2 amplified with HyF and HyalR; Lane 10, 10 μ L of Negative control; Lane 12, Empty.

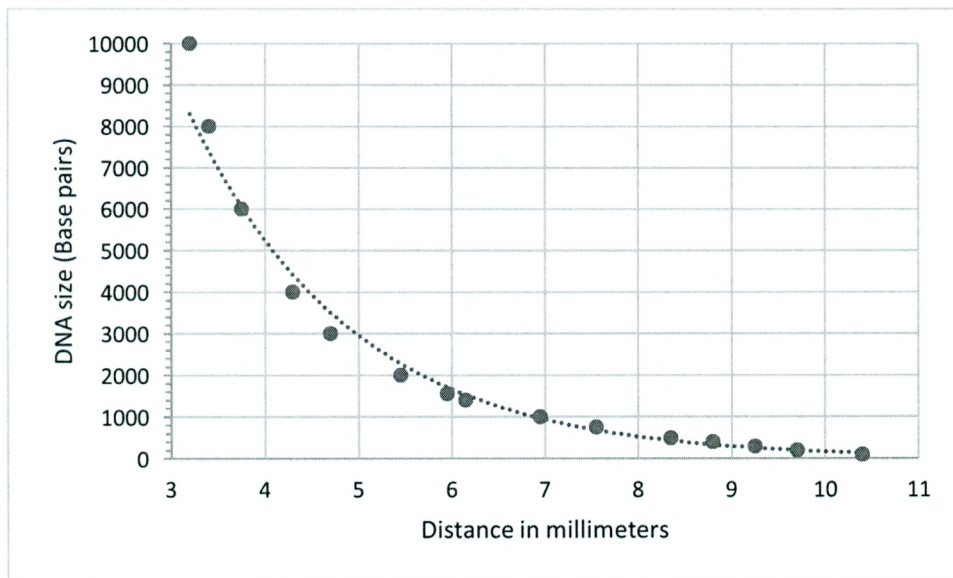


Figure 9. Standard curve generated by electrophoretic separation of HiLo ladder (Minnesota Molecular) fragments. The DNA sizes for this DNA size ladder range from 10,000 bp to 50 bp.

A recent invasion of a hydrozoan, *Gonionemus vertens*, into New Jersey coastal waters this past summer (Gaynor et al., 2016) provided an opportunity to test our hyaluronidase primers on gDNA from this species. Figure 10 illustrates our amplification of hyaluronidase gene from *G. vertens* gDNA. Using four different combinations of primers I was able to get amplification but I was not able to produce a clean, single band suitable for sequencing. In all reactions I saw multiple bands generated. This suggests two things: 1) that the hyaluronidase gene is present in *G. vertens*; and 2) that it likely to be present as a multi-gene family based on the size and numbers of amplicons seen. I cannot rule out the possibility that some of these amplicons may be due to non-specific hybridization of primers within the *G. vertens* genome resulting from the lower annealing temperatures used in this experiment. Since this was outside of the initial scope of this project, I did not attempt to purify or sequence any of these amplicons.

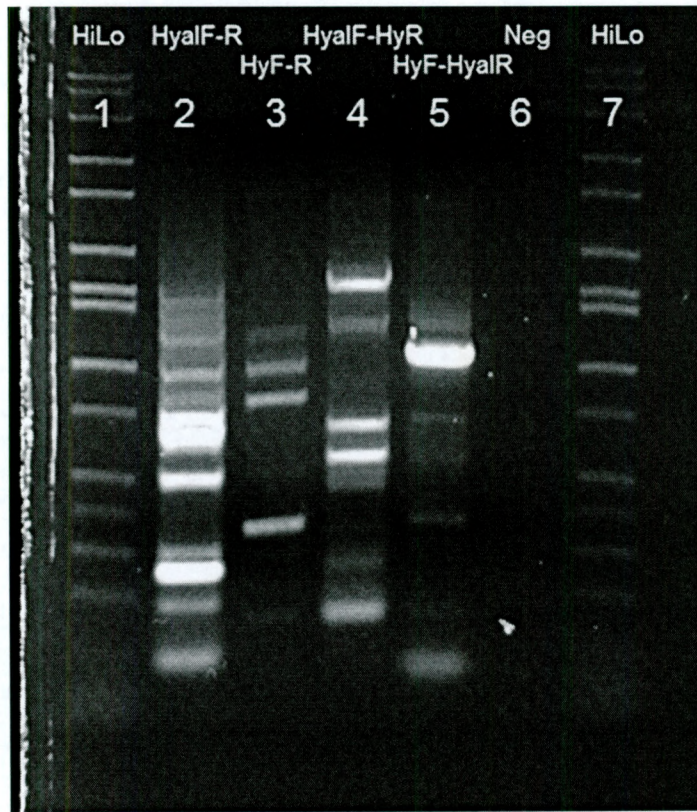


Figure 10. *Chrysaora quinquecirrha* hyaluronidase primers used to amplify *Gonionemus vertens* hyaluronidase. Due to the intensity and frequency of the multiple bands per amplicon, sequencing was not possible. Lane 1 & 7, 10 μ L of Hi Lo DNA Ladder (Minnesota Molecular, Inc., www.mnmolecular.com); Lane 2, 10 μ L of DNA from GV1 amplified with HyalF and HyalR; Lane 3, 10 μ L of DNA from GV1 amplified with HyF and HyR; Lane 4, 10 μ L of DNA from GV1 amplified with HyalF and HyR; Lane 5, 10 μ L of DNA from GV1 amplified with HyF and HyalR; Lane 6, 10 μ L of Negative control.

For the amplicons generated from *Chrysaora quinquecirrha*, sequencing of the fragments typically produced electropherograms with *ca.* 700 bases from either end of the fragment, which were then grouped using Geneious R10 according to the primer they were derived from. HyalR generated many low quality sequences (Figure 11), with no overlaps to HyalF, but the collected

higher quality sequences were aligned (Figure 12). HyalF likewise also generated many low quality sequences, with no overlap on either HyalR's sequences or the mRNA sequence (Figure 13). They did however, have internal consistency allowing the higher quality sequences to be aligned (Figure 14). The inner sequences generated by HyF and R featured semi-consistent overlaps, sorted as 3 different homologous groups, with group 1 containing primarily TR2 sequences and no insertion (Figure 15), group 2 containing primarily TR1 sequences and the insertion sequence (Figure 16), and group 3 containing both TR1 and 2 sequences and an inconsistent region for its intron (Figure 17).

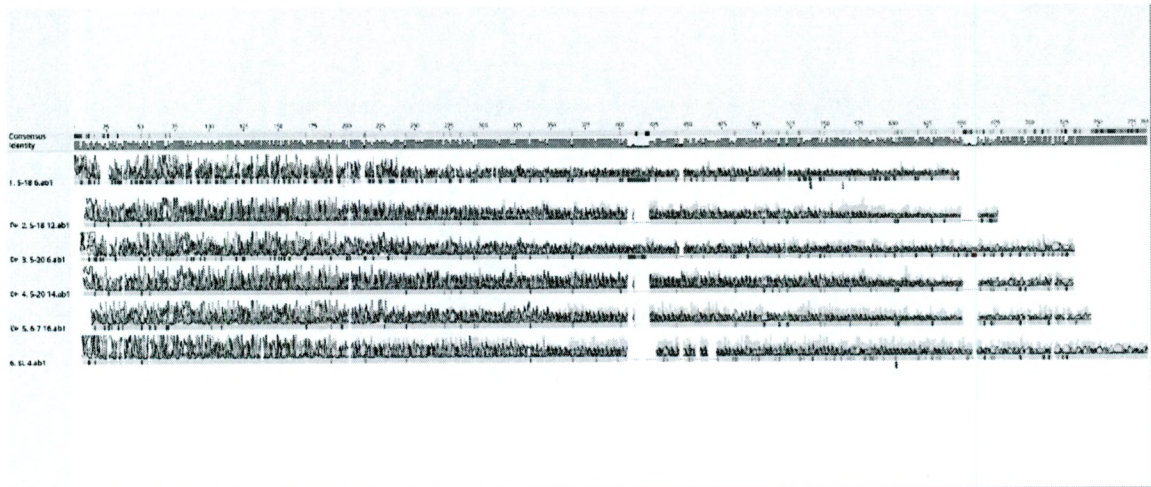


Figure 11. Electropherograms of HyalR generated sequences prior to manual base call edits and gap deletions. Low quality sequences were excluded.

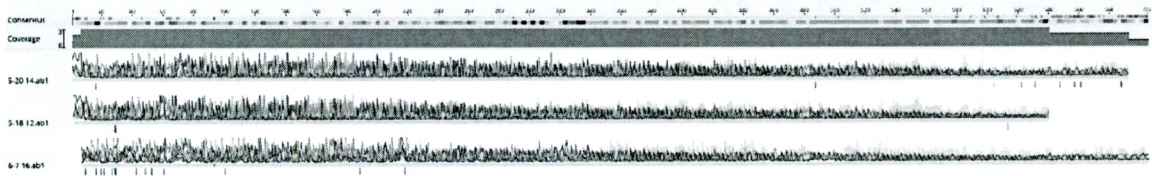


Figure 12. Electropherograms of HyalR generated sequences after manual base call edits and gap deletions. Divergent sequences from Figure 11 were excluded.

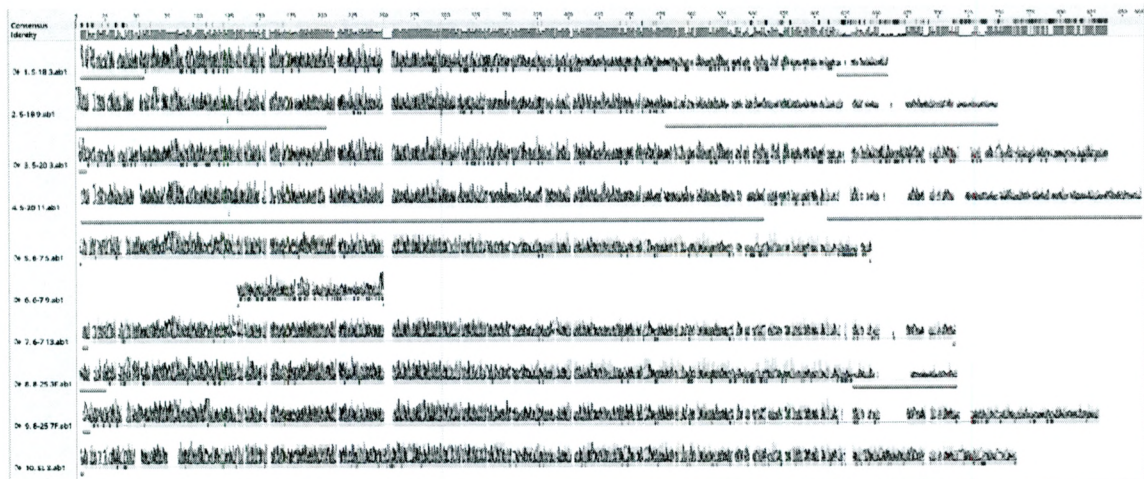


Figure 13. Electropherograms of HyalIF generated sequences prior to manual base call edits and gap deletions. Low quality sequences were excluded. Pink annotations denote automatically trimmed sequences below the automated quality threshold.

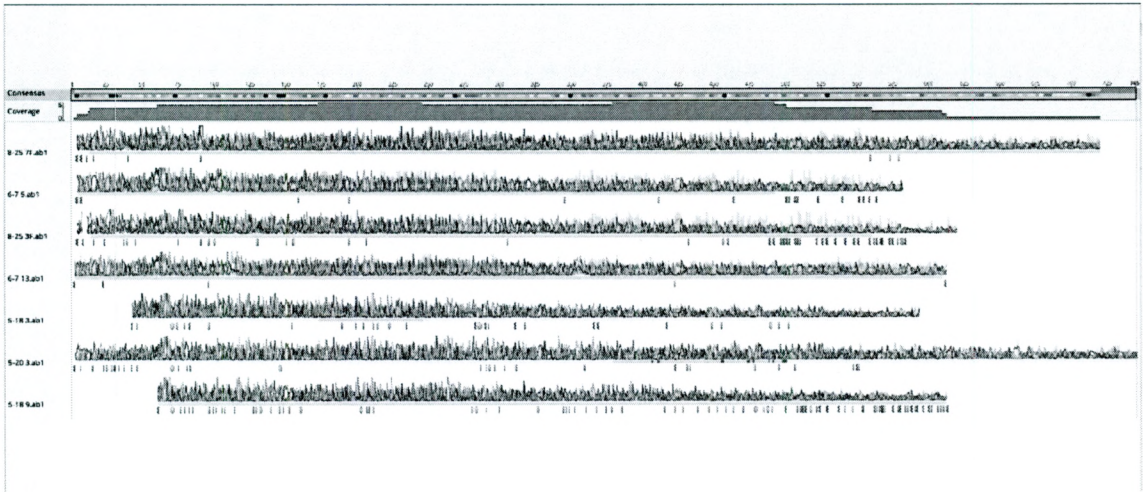


Figure 14. Electropherograms of HyalF generated sequences after manual base call edits and gap deletions. Divergent sequences from Figure 13 were excluded.

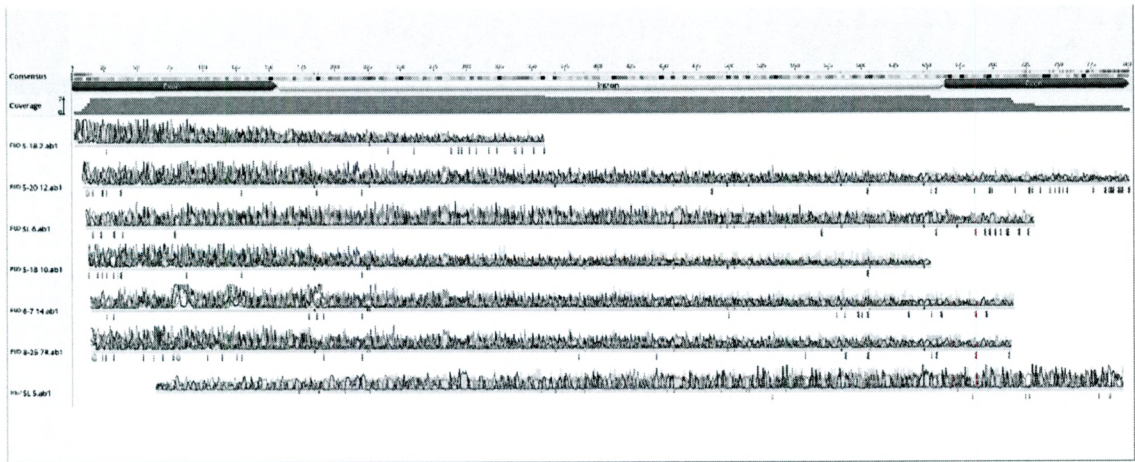


Figure 15. Electropherograms of HyR and HyF generated sequences, homologous group 1 of 3. Exon regions are annotated in black and the intron in white. Manual base call edits and gap deletions have been made. The intron is approximately 500 base pairs long.

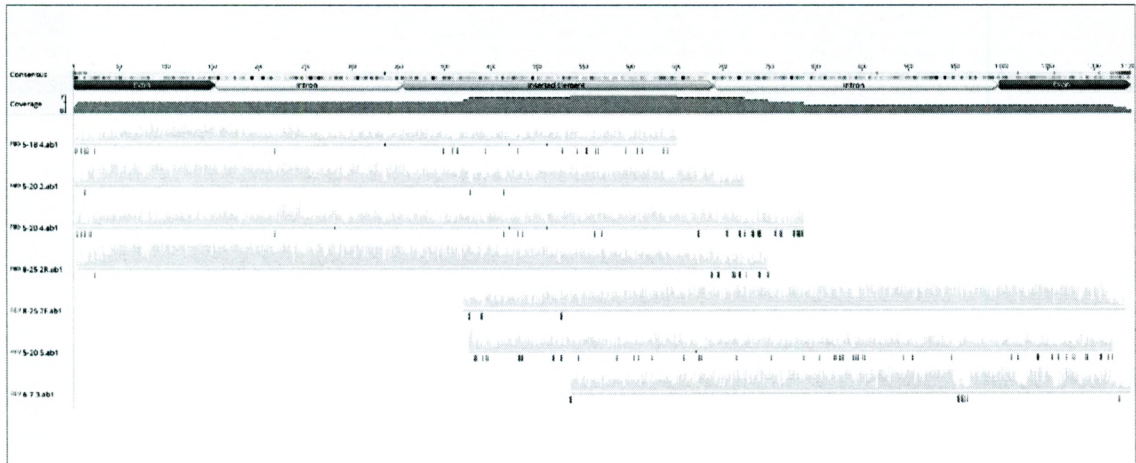


Figure 16. Electropherograms of HyR and HyF generated sequences, homologous group 2 of 3. Exon regions are annotated in black, intron in white and insertion in gold. Manual base call edits and gap deletions have been made. The intron is approximately 500 base pairs long without the insertion sequence, which is approximately 320 long. Electropherograms have been color reduced due to size.

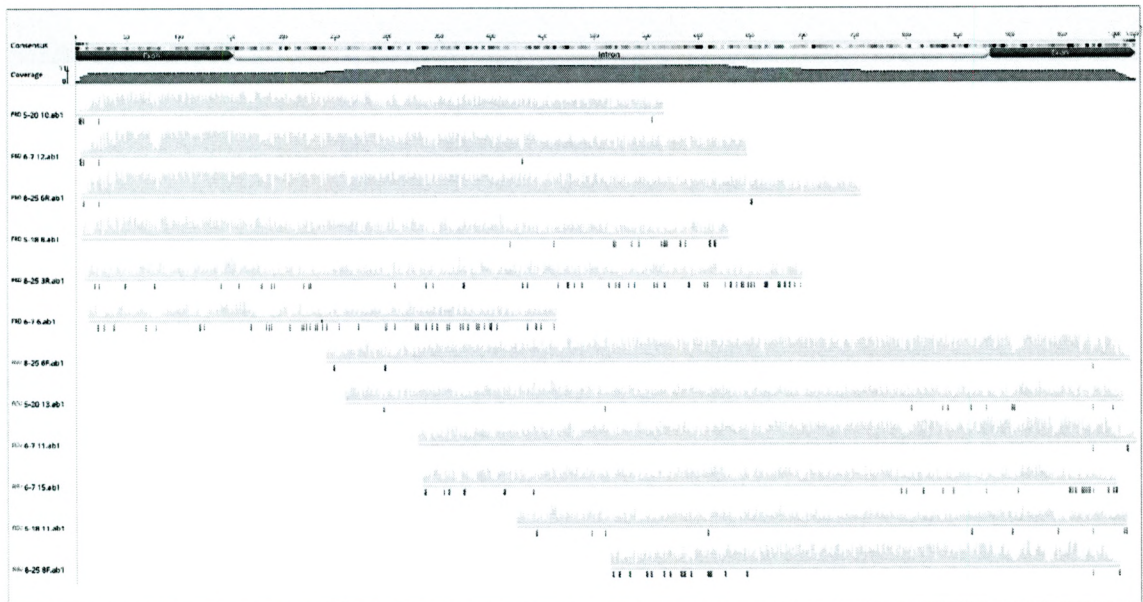


Figure 17. Electropherograms of HyR and HyF generated sequences, homologous group 3 of 3. Exon regions are annotated in black and the intron in white. Manual base call edits and gap deletions

have been made. The intron is approximately 720 base pairs long. Electropherograms have been color reduced due to size.

III. Evidence for Introns in the Hyaluronidase Gene from *Chrysaora quinquecirrha*

Since HyalR-F were located only 674 bases apart based on the RNA-Seq data, overlap was expected from the generated sequences. The individual sequences were aligned using Genious R10 and manually corrected and edited where necessary, creating consensus sequences approaching the true DNA sequence. These consensus sequences were long enough to have nearly a complete overlap of each other, yet failed to reach any overlap. After new sequences were generated from HyR-F and overlaid into a consensus, an overlap was reached, but again after a longer distance than anticipated. When the consensus DNA sequences were aligned with the RNA sequence, the RNA featured uninterrupted sequences of homology not reflected in the DNA (Figure 18) with the exception of the Hyal F sequences which featured no overlaps at all. HyalF's binding site is only 36 bases downstream from the start of HyF's homologous sequence however, despite being over 600 bases downstream in its consensus DNA sequence. The inner sequences in particular featured these gaps, which maintained internal consistency and created overlaps between the pairs. While HyR-F created 3 consensus groups, when aligning only the exons, the separate groups become homologous with each other and with the RNA seq (Figure 19). The total assembled DNA currently extends from the binding site of HyalR to the start of the HyF binding site and contains two introns, with another intron immediately following the HyF binding site. It spans 677 bases of mRNA and 1984 of gDNA, owing its disparity to the 464 base forward intron and the 843 base inner intron, which itself contains a 335 base insertion sequence. The rear intron found in HyalF's sequences has not yet been fully characterized, but can be identified as being at least 728 bases long due to the lack of homology with the mRNA.

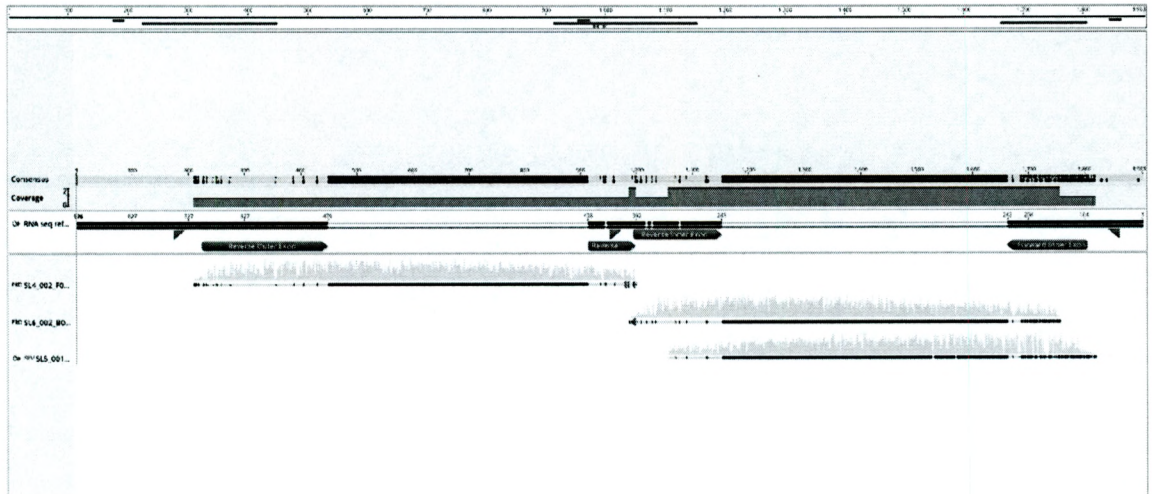


Figure 18. The first four sequences generated from the initial runs of each primer, HyalR, HyR and HyF from top to bottom. HyalF is not shown as it has only tentative overlaps at the 3' extension, which were too low quality for the program to include.

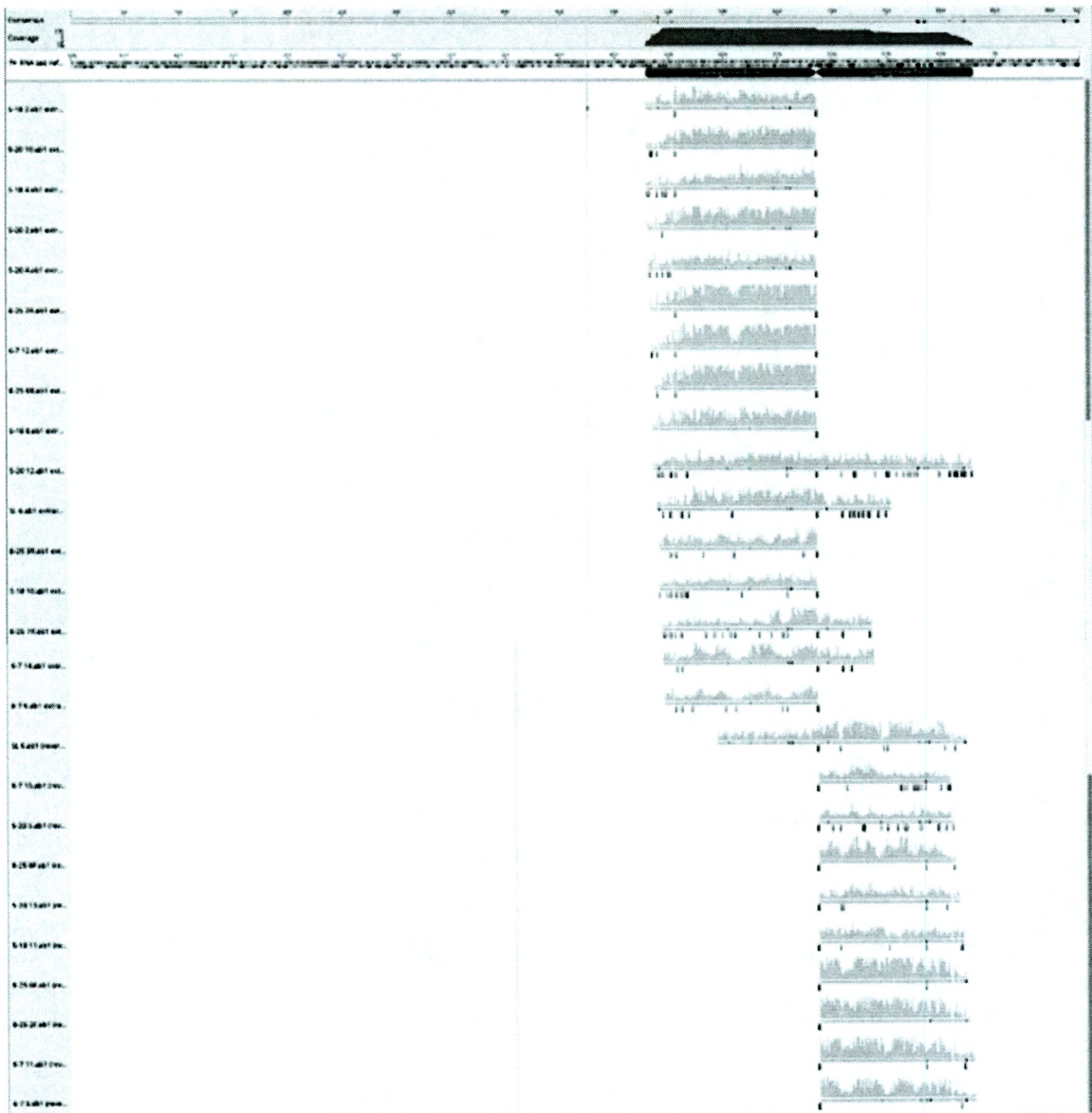


Figure 19. HyR-F exon alignment without any potential intron sequence. All 3 homologous groups are present.

IV. Insertion Sequence within Intron

The three homologous groups in the HyR-F sequences indicate a sequence found exclusively in TR1 gDNA (Figure 20). This sequence has high intra-group homology and is bordered by high intergroup homology, but is entirely absent in the other groups. The ends of the insert are 38 bases long and with minor edits, can be made into perfect inverted repeats. The 5' end is GGGCGTATTTTTTTGGTTACCTCCTGTTTTTAGCAGAC while the reverse of the 3' end is CCCGCATAAAAAAACCWGTGTAAGACAAAAGTCGTCTG which was edited into CCCGCATAAAAAAACCAATGGAGGACAAAATCGTCTG in order to create the perfect repeat (Figure 21). Since this section of the DNA has only a few sequences, this section could have much higher error than the exons or introns, potentially allowing this level of error to occur. Further sequencing of this region with closer primers will create a more confident idea of the size of the repeated ends.

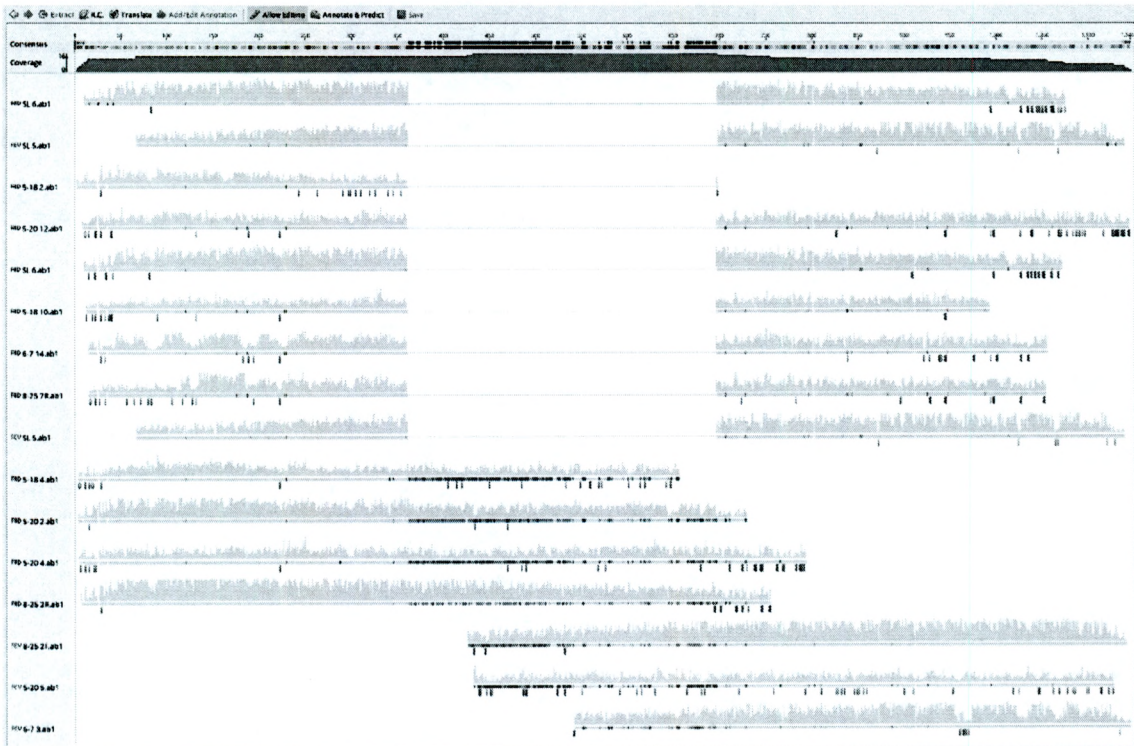


Figure 20. Alignment of homologous groups 1 and 2 together. Homologous group 2 contains mostly TR1 sequences, where group 1 contains mostly TR2. Group 3 contains an even distribution, but contains a non-homologous region in its intron as compared to both other groups. The gap found in group 1 indicates the insertion in group 2.

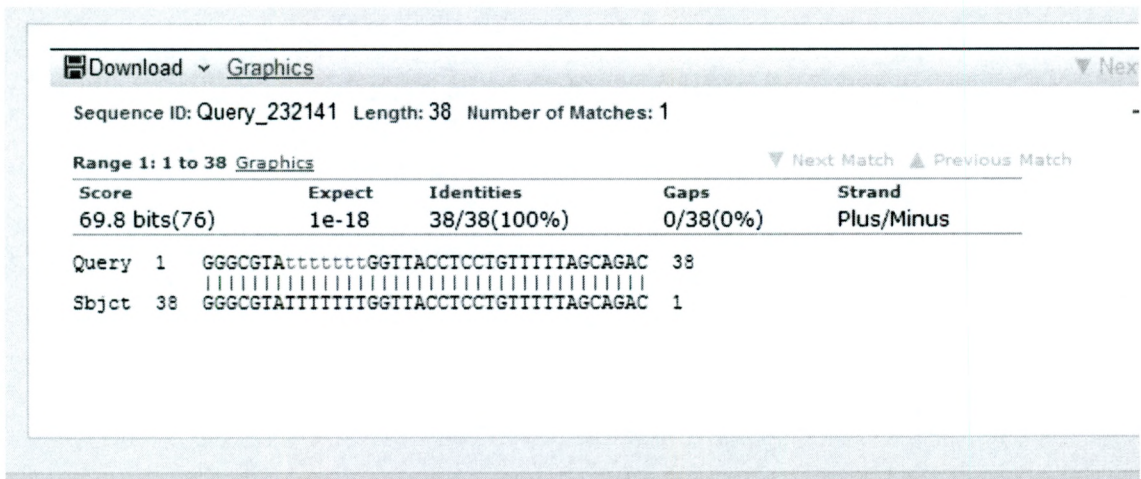


Figure 21. Inverted repeats from the insertion sequence. The 5' end was left unedited out to 38 bases then truncated. The 3' end was taken from 39 bases before the terminus of the insertion sequence, and edited. An adenine was deleted from a polyA run and the lowercase letter indicate base call changes. These two sequences were blasted against each other and form perfect inverted sequences.

V. Hyaluronidase Activity

The activity of both the bovine testicular hyaluronidase and purified cnidocysts was detected at low concentrations. *Chrysaora quinquecirrha* purified cnidocysts contain an unknown concentration of hyaluronidase, so raw lysate does not create an accurate representation of enzyme concentration. However, as lysate concentration increases, ideally the entirety of its contents concentration increases. Therefore, the lysate can be used as an indicator of hyaluronidase due to its increased hyaluronic activity over a greater concentration of the lysate.

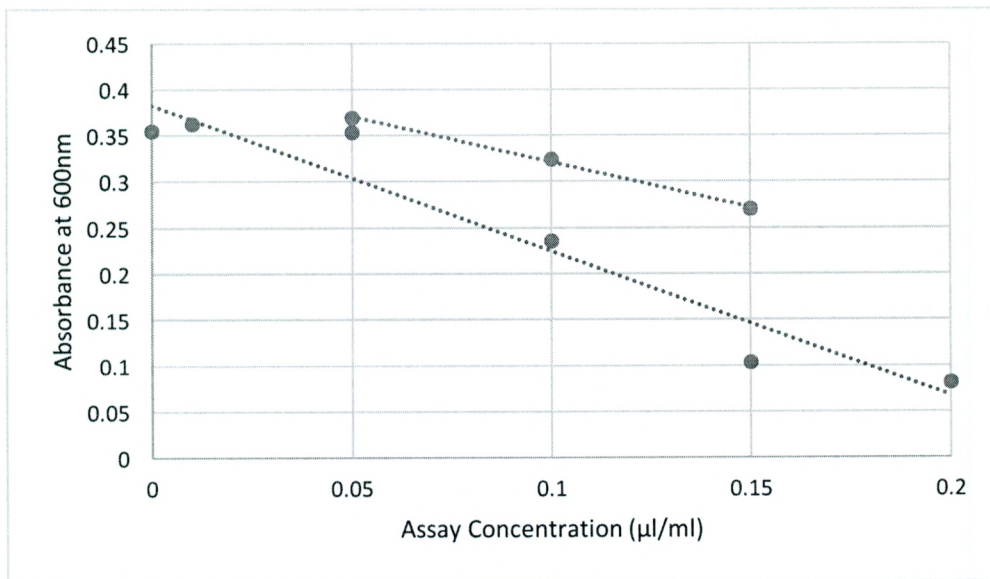


Figure 22. Low concentration standard curves for bovine testicular hyaluronidase (Blue) and *Chrysaora quinquecirrha* purified cnidocyst extract (Red) incubated for 45 minutes. All samples were blanked with an equal volume of deionized water prior to measurement. Bovine testicular hyaluronidase assay volume is 0.025µg/ml enzyme solution. For the purified cnidocysts, actual enzymatic concentrations were unknown, and the assay volume is just purified cnidocyst lysate.

VI. Homology

Attempting to align multiple hyaluronidase proteins in CLUSTAL Omega indicates the relative distance between the species in each group. Group 1 (Figure 23) is built from *Chrysaora quinquecirrha*, *Hydra vulgaris* and typical highly sequenced organisms such as *Mus musculus* and *Homo sapiens*. Of these, *Crotalus adamanteus*, the eastern diamondback, was the closest match to *Hydra vulgaris* and *Chrysaora quinquecirrha*, as well as the only other member to use hyaluronidase in its venom rather than in fertilization. Group 2 (Figure 24) was comprised of species in the NCBI database with high homology to the BLASTX of contig 20047. Here, both *Chrysaora quinquecirrha* and *Hydra vulgaris* are more homologous to *Acropora digitifera* than to

the chordates, but *Hydra vulgaris* remains the closest relative to the RNA sequence from *Chrysaora quinquecirrha* as it stands.

The active site of hyaluronidase is a glutamic acid located at 131 in human hyaluronidase, marked in Figures 23 and 24 by a double arrow. Throughout all the present hyaluronidases, this site remains homologous even between highly distant phylogeny. The other arrows present indicate catalytic secondary sites that help bind hyaluronic acid, also conserved between all presented species.

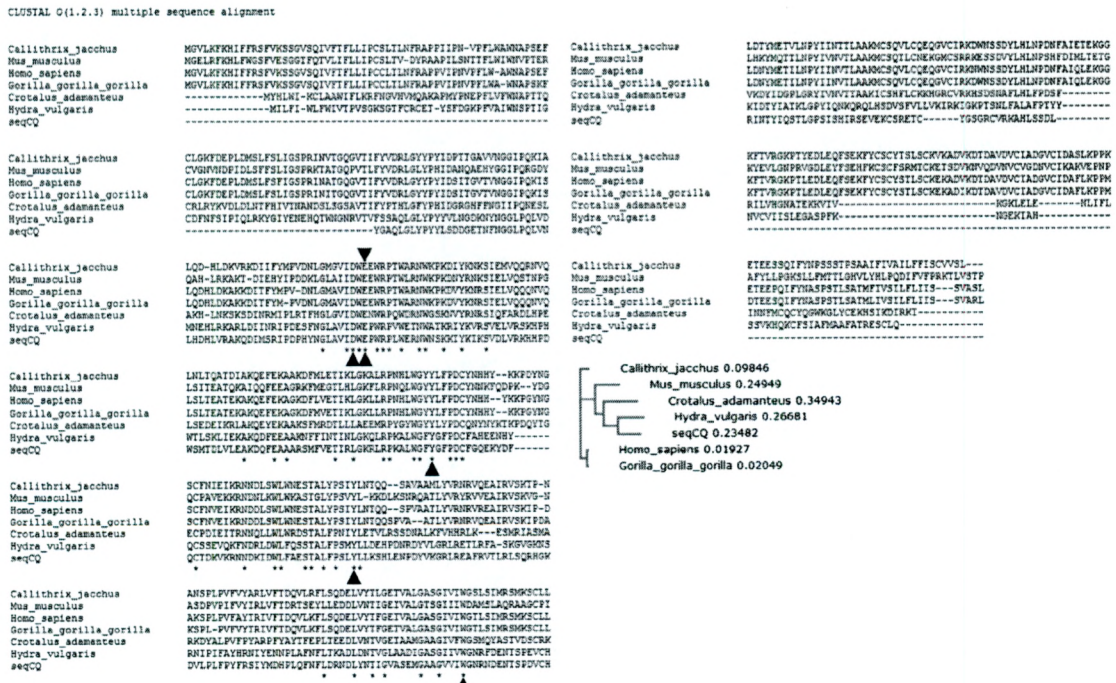


Figure 23. Clustal alignment of *Chrysaora quinquecirrha*, *Hydra vulgaris* and several chordates' hyaluronidase. *Crotalus adamanteus* is the only chordate listed that uses the enzyme as venom rather than for fertilization. Arrows indicate sites of catalytic importance, with the double arrow indicating the active site.

CLUSTAL O(1.2.3) multiple sequence alignment

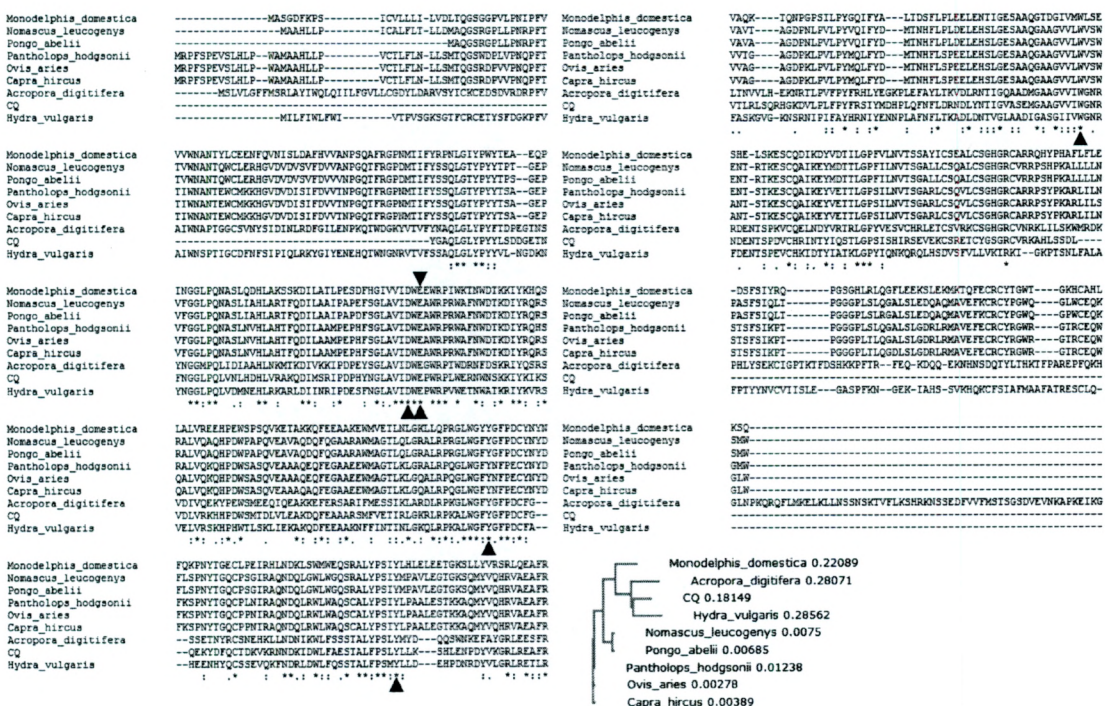


Figure 24. CLUSTAL Omega alignment of *Chrysaora quinquecirrha*, *Hydra vulgaris* and more closely related hyaluronidase genes. *Acropora digitifera* had its sequence truncated as it extended far beyond all of the other lengths. Arrows indicate sites of catalytic importance, with the double arrow indicating the active site.

Discussion

I. Evidence for Hyaluronidase Expression in the *Chrysaora quinquecirrha* Transcriptome

Based on the assembled contigs obtained from the *Chrysaora quinquecirrha* RNA-Seq library, a series of BLASTX searches were performed to find significant matches to known proteins in the NCBI database. One such sequence, contig 20047, appeared to contain a possible hyaluronidase gene. When BLASTed against the database, a match to the hyaluronidase 1-like protein from *Hydra vulgaris* was found, along with many other matches for hyaluronidase 1-like proteins. *Hydra vulgaris* is 56% identical to the mRNA sequence, and the other matches range from 51 to 43%, but they all cover nearly the entire query, 91% at the lowest. Since *Hydra vulgaris* is a hydrozoan, which is a type of medusozoan like *Chrysaora quinquecirrha*, a scyphozoan, it stands to reason that they would share high homology. Furthermore, when matching the *Chrysaora quinquecirrha* sequence to the *Hydra vulgaris* sequence, the homology starts 79 amino acids into the *Hydra vulgaris* sequence and ends before the completion of the sequence. While some of this can be attributed to minor variations in the amino acids, the more telling aspect is that the protein sequence from *Chrysaora quinquecirrha* is likely to be incomplete. In fact, I estimate that I have approximately 64.22% of the protein encoded in this contig, based on the corresponding protein size found in *Hydra vulgaris*. To determine this, the RNA would have to be extended from each end, or the bordering contigs would need to be found to extend this sequence. Either way, the true, complete sequence of this gene will require the DNA sequence rather than the RNA, which was determined as part of this research.

II. Hyaluronidase Gene Structure from *Chrysaora quinquecirrha*

With the close relation between *Hydra vulgaris* and *Chrysaora quinquecirrha*, it is likely that the overall protein will maintain its tertiary structure between the two. The only way to prove this would be to either crystallize the CQ protein, or to complete the sequence and see if its homology is high enough to allow for predictive folding using HV's hyaluronidase as a template. The anthozoan *Arcopora digitifera*'s hyaluronidase is 199 amino acids longer, nearly all of which are downstream of the terminus of HV's hyaluronidase, as well as the chordate hyaluronidases. As such, it's unlikely that the CQ will follow that trend. However, HV's intron distribution in its hyaluronidase gene is very different from what has been characterized in CQ thus far (Chapman et al., 2010). Hydra has seven introns of immensely divergent size, ranging from *ca.* 20,000 base pairs to only *ca.* 100 base pairs. The two fully characterized CQ hyaluronidase introns are far more regular, being *ca.* 400 and *ca.* 700, fitting neither of the extremes found in the HV hyaluronidase gene. Interestingly, the AD hyaluronidase gene has much closer intron arrangement, with 5 introns ranging from *ca.* 1600 to *ca.* 280 (Shinzato et al., 2011). The final exon is also much longer than any others in the gene, encompassing the additional length the encoded protein has over HV's hyaluronidase. As far as CQ is concerned, the current intron placement does not perfectly align with either of its closest relatives, so the genetic structure will require extension of the sequenced regions to be fully determined. As a comparative effort, *Gonionemus vertens* samples were also amplified with the CQ hyaluronidase primers I had available. Since GV is also a hydrazoan, I had hoped it might be similar in its intron layout to either HV or CQ, possibly providing a middle ground between the two genetic layouts. However, the primers reacted far too non-specifically, and amplified several bands per pair (Figure 7). These would be impossible to sequence properly, but did show how close the sequences between CQ and GV are, or even indicated the presence of a hyaluronidase gene in GV as well, but that remains to be determined.

III. Evidence for Introns in the Hyaluronidase Gene from *Chrysaora quinquecirrha*

Since the RNA sequence does not include introns, the size disparity between it and the DNA sequence would suggest that non-coding sequences are present in the DNA of *Chrysaora quinquecirrha* hyaluronidase. Introns are very common in eukaryotic genomes, and are the easiest explanation for non-coding DNA (Kim et al., 2007). However, the size disparity does not suggest where the introns would be located, only that they are between the initial outer primers, HyalF-R. Since these primers have known locations on the RNA sequence, they can be an anchor point for the size disparity, as shown on Figure 4. The inner primers, however, do not have a known location since they were developed from the non-overlapping sequences of the outer amplicons. The reverse inner primer, HyR, is very similar to a known region of the RNA sequence, and it is likely that the primer inadvertently incorporated errors from the DNA sequencing which masked its appearance on the RNA sequence. This location was found 295 bases away from HyalR, easily within the region of legibility for the sequence. However, HyR was generated from the 3' end of the legible region of the HyalR sequence, 713 bases apart from the beginning of the sequence. This sequence begins its homology 26 bases away from the 3' terminus of HyalR, leaving 444 bases unaccounted for in the RNA. Upon examining the sequence for its homology, there is a gap in the sequence 464 bases long that does not correlate with the RNA sequence. The RNA matches to the 5' and 3' bordering regions of the gap perfectly, indicating that this gap is likely an intron. Furthermore, the gap itself begins with a guanine (G) and thymine (T) then ends with an adenine (A) and guanine (G), another marking of an intron (Mount, 1982). While the exact sizes don't match up, this is possibly attributed to errors in the intron sequence, as a 20 base disparity across a 713 base sequence is reasonably attributed to error in the electropherograms base calling, which becomes increasingly likely as the sequence is read further down the 3' end.

The other inner primer, HyF, regrettably does not have an anchor point as reliable as HyR. The outer sequence from HyalF has no homology until the very end of the legible region, 727 bases

into the sequence. At this point, the sequence is more prone to error, but with corroborating base calls from additional sequences, consensus sequences can be extended into this region. The RNA sequence matches the 3' end of the HyalF sequence on the same base that HyF has on its 3' end. While a single base is 25% likely given random assortment, and such a weak point is hardly convincing data, it provides a possible point for a future anchor, and an explanation for the size disparity between the RNA and DNA distances between HyalF and HyF. If this base is true and this is the location of the HyF primer, then the 3' end of HyalF would be 2 bases deep into the 5' end of HyF. However, HyF was developed from the HyalF sequence 708 bases into the sequence. While the 5' end of the sequence remains unanchored, it was generated from a known location on the RNA, which will serve as its anchor point for the purposes of size. Further primers will be needed to determine the outer end of this intron. Since there is a matching end for the sequence, the size of the intron can be inferred by the disparity between the DNA and RNA distances between the match and the primer, which are 17 bases for the RNA and 727 for the DNA, indicating an unaccounted 710 bases likely belonging to one or more introns in the region.

Within the inner sequence, there is another size disparity, as the DNA bands on the electrophoresis gel indicated. Based on the RNA, the two primers would only be 341 bases apart, but the DNA tells that they are 850 bases apart, leaving 509 bases unaccounted for. HyR and F have overlapping sequences and overlap with homology in the RNA clearly up until a specific point, where a large gap 508 bases in length is located. While not a perfect match, this gap is clearly a fit for the unaccounted bases. This gap, much like the HyalR intron, is bordered by RNA homologous regions that do not break sequence in the RNA and are led by a guanine and thymine, then ends with an arginine and guanine.

The overall length of the DNA with introns becomes 2378, with potential for error more likely in the introns due to lack of corroborating RNA lengths. This does not match the gel accurately, but the range of error on the gel increases with DNA size.

IV. Insertion Sequence within Intron

Within homologous group 2, an additional insertion sequence is present, as seen in Figure 13. This 334 base insertion behaves much like the intron it's located in, with it creating a gap in homology between homologous group 2 and 1. Both sides of the gap are bordered by intron sections homologous with group 1's introns without break. In Figure 14, the inserted gap sequence is shown in alignment to homologous group 1 and 2, which breaks for the duration of the insert. The ends of the insert are also palindromic 17 bases in, or 38 bases in allowing for 6 base errors. While 6 errors in so short a space are less likely for a consensus sequence, the limited number of sequences with this insert, 7 in total, does allow for less certainty with any given base. Most previously identified insertion sequences are bordered by inverted repeats of 10 to 40 bases (Mahillon and Chandler, 1998). Most curiously is that this insertion is conserved in homologous group 2, but absent from 1 or 3, possibly as a result of group 2 being mostly TR2 sequences and 1 being mostly TR1 sequences. It's possible the sequence is merely a novel insertion into TR2's genome or that it is a locally inserted sequence found in specific regions of the jellyfish that TR2 retained more than TR1. The internal sequence was blasted against the NCBI database and found very little to match with, so its function, if any, remains unknown at this time. Further sequencing of this region will hopefully provide more sequences with this insertion that provide a better consensus of the sequence and the exact size of its palindromic ends.

V. Hyaluronidase Activity

While the RNA and prior research (Long-Rowe and Burnett, 1993) suggests that hyaluronidase is present in *Chrysaora quinquecirrha*, an enzymatic assay would further reinforce the idea that the protein is both present and active. The standard enzymatic assay for hyaluronidase utilized purified bovine testicular hyaluronidase 1, which reacts with hyaluronic acid to prevent it from releasing sodium from a solution containing sodium acetate. The release of sodium does not occur naturally at the pH and temperature hyaluronidase is most active at, allowing for the normally

difficult to observe process of hyaluronic acid breakdown to be visually quantifiable by spectrophotometry. The solution has its highest absorbance at 600 nm, and the cloudiness of the solution is quite visually apparent. At high concentrations, the process is exponentially limiting, likely a product of the saturation of the enzyme (Figure 21). At a certain point, adding more of the enzyme no longer causes a proportionally equal amount of hyaluronic acid to break down due to the unlikeliness of the encounter. At lower concentrations however, the relationship between the concentration and the absorbance appears more linear (Figure 22). At extremely low concentrations, the absorbance actually increases above untreated hyaluronic acid, possibly due to an additive in the hyaluronidase solution.

Unfortunately, due to the methods used for *Chrysaora quinquecirrha* hyaluronidase, the actual specific activity of the enzyme cannot be determined at this time. The standard has a known concentration for all of its tests, allowing for an activity in turbidity reducing units (TRU) to be applied to it. The *Chrysaora quinquecirrha* hyaluronidase does not have a known concentration, as it was obtained from purified cnidocysts that were sonicated to release all of their content. How many other proteins were present in the cnidocysts remains unknown and the concentration of hyaluronidase amongst the other components of the sonicate is also a mystery. In a purification method for bee hyaluronidase, it was observed that pure hyaluronidase had an 1143 fold increase in specific activity over raw venom extracts, suggesting that hyaluronidase only occupies approximately 0.1% of the native venom (Kemeny et al., 1984). While honey bees and Sea nettles are distantly related, the role hyaluronidase plays would not indicate a vast difference in the concentration in their respect host's venom. Furthermore, there is no way to know how much hyaluronidase was denatured by the storage process or the sonication, or even lost in the transfer. Despite all this, there is clear evidence of activity, as the increased concentration of the sonicate correlates with a linear regression in absorbance, albeit with lesser slope than the standard. At the very least, it would appear that the cnidocysts do indeed have hyaluronidase activity, which I can

infer that this protein is a component of the sea nettle's venom. It remains to be determined, however, if *Chrysaora quinquecirrha* contains more than one type of hyaluronidase.

VI. Homology

Initially, *Hydra vulgaris* was the closest match to *Chrysaora quinquecirrha* hyaluronidase in the NCBI database, and in performing a CLUSTAL Omega alignment with various chordates, it remains true (Figure 23). However, it is worth noting that the closest match between the cnidarians and the chordates is *Crotalus adamanteus* (Eastern Diamondback rattlesnake), which is the only chordate amongst that list to use the hyaluronidase as a venom rather than a sperm adhesion molecule. Even with the massive gulf between the cnidarians and the other groups, there are still some conserved regions among all of the hyaluronidase sequences.

The more closely related species in Figure 24 have better homology, with *Hydra vulgaris* still the most closely related and homologous protein. *Acropora digitifera* (Arcoporidae Coral) is the next closest, as one might expect from an anthozoan. Both of these species lack metabolic hyaluronidases or hyaluronic acid, meaning that their hyaluronidase proteins are used as venom like in *Chrysaora quinquecirrha*. The remaining species are far more closely related to each other than to the rest of the group. Since they are non-venomous chordates, it stands to reason that their metabolic hyaluronidases would be moderately divergent from the venom hyaluronidases. While distantly removed from the primates, the fact that there is a correlation is likely due to the universal structure of hyaluronic acid.

The active site of hyaluronidase is a single amino acid, glutamic acid (E) 131 in human hyaluronidase 1 (Stern and Jedrzejewski, 2006). Figure 18 shows conservation of this glutamic acid, as well as Asp129, Tyr202, Tyr247 and Trp321, other residues vital for the stabilization of hyaluronic acid for digestion, throughout the species listed despite the phylogenetic distance. While the structure of the protein may shift slightly from changes in the sequence, these residues are

critical to the function of hyaluronidase, and as such, have been conserved throughout the evolutionary process. Since the hyaluronidase gene and the putative translation product found in *Chrysaora quinquecirrha* also contains these active and secondary sites, it's highly likely to also be a hyaluronidase.

Conclusion

Chrysaora quinquecirrha has been previously proven to contain hyaluronidase (Long-Rowe and Burnett, 1993), which was located in mRNA sequencing and amplified into gDNA using primers drafted from contig 20047. The amplification produced segments of approximately 2300 base pairs, rather than the anticipated 674 bases between the primers on the mRNA. From these initial sequences, internal primers were designed which generated still yet larger segments, approximately 1100 base pairs. Though sequencing the segments and aligning them in Geneious R10, two introns, of 464 and 842 bases respectively, were discovered. Within the second intron, an insertion sequence present in only a single specimen was also discovered. This sequence is 335 bases long and features inverted repeated sections at its termini, but remains less accurate than the other areas of DNA due to the limited sequences containing the insert. Hyaluronidase assays performed on *Chrysaora quinquecirrha* cnidocysts observed the presence of hyaluronidase activity, in corroboration with prior research. The putative protein encoded by contig 20047 conserves the active site and accompanying secondary sites of human hyaluronidase, which remain conserved in order to continue digesting the equally unchanging hyaluronic acid polymer. Efforts are continuing to extend and complete the sequence of the full length gene.

Literature Cited

- Altschul S. F., Madden T. L., Schäffer A. A., Zhang J., Zhang Z., Miller W., Lipman D. J. (1997). Gapped BLAST and PSI-Blast: a New Generation of Protein Database Search Programs. *Nucleic Acids Research*. 25:3389-3402.
- Anderson P. A. V., Bouchard C. (2009). The Regulation of Cnidocyte Discharge. *Toxicon*. 54:1046-1053.
- Cegolon L., Heymann W. C., Lange J. H., Mastrangelo G. (2013) Jellyfish Stings and Their Management: A Review. *Marine Drugs*. 11:523-550.
- Chapman J. A., Kirkness E. F., Simakov O., Hampson S. E., Mitros T., Weinmaier T., Rattei T., Balasubramanian P. G., Borman J., Busam D., Disbennett K., Pfannkoch C., Sumin N., Sutton G. G., Viswanathan L. D., Walenz B., Goodstein D. M., Hellsten U., Kawashima T., Prochnik S. E., H. Putnam N. H., Shu S., Blumberg B., Dana C. E., Gee L., Kibler D. F., Law L., Lindgens D., Martinez D. E., Peng J., Wigge P. A., Bertulat B., Guder C., Nakamura Y., Ozbek S., Watanabe H., Khalturin K., Hemmrich G., Franke A., Augustin R., Fraune S., Hayakawa E., Hayakawa S., Hirose M., Hwang J. S., Ikeo K., Nishimiya-Fujisawa C., Ogura A., Takahashi T., Steinmetz P. R. H., Zhang X., Aufschnaiter R., Eder M., Gorný A., Salvenmoser W., Heimberg A. M., Wheeler B. M., Peterson K. J., Böttger A., Tischler P., Wolf A., Gojobori T., Remington K. A., Strausberg R. L., Venter J. C., Technau U., Hobmayer B., Bosch T. C. G., Holstein T. W., Fujisawa T., Bode H. R., David C. N., Rokhsar D. S., Steele R. E. (2010) The Dynamic Genome of Hydra. *Nature*. 464:592-596.
- Chao K. L., Muthukumar L., Herzberg O. (2007) Structure of Human Hyaluronidase-1. A Hyaluronan Hydrolyzing Enzyme Involved in Tumor Growth and Angiogenesis. *Biochemistry*. 46:6911-6920.
- Dorfman, A. (1955) *Methods in Enzymology*, 1:166-173.
- Fautin D. (2009) Structural Diversity, Systematics and Evolution of Cnidaria. *Toxicon*. 54:1054-1064.
- Fox J. W. (2013) A Brief Review of the Scientific History of Several Lesser-Known Snake Venom Proteins: L-Amino Acid Oxidases, Hyaluronidases and Phosphodiesterases. *Toxicon*. 62:75-82.
- Frazao B., Vasconcelos V., Antunes A. (2012) Sea Anemone (Cnidaria, Anthozoa, Actiniaria) Toxins: An Overview. *Marine Drugs*. 10:1812-1851.
- Gacesa P., Civill N. D., Harrison R. A. P. (1994). PH-20 and Sperm Hyaluronidase: a Conceptual Conundrum in Mammalian Fertilization. *Biochemical Journal*. 303:335-336.
- Gaynor J. J., Bologna P. A. X., Restaino D., Barry C. L.. (2016) First Occurrence of the Invasive Hydrozoan *Gonionemus vertens* A. Agassiz, 1862 (Cnidaria: Hydrozoa) in New Jersey, USA. *Bioinvasions Records*. 5(4):233-237.
- Girish K. S., Kemparaju K.. (2005) Inhibition of *Naja naja* Venom Hyaluronidase by Plant-Derived Bioactive Components and Polysaccharides. *Biochemistry (Moscow)*. 70(8): 948-952.

- Gmachl M., Kreil G. (1993). Bee Venom Hyaluronidase is Homologous to a Membrane Protein of Mammalian Sperm. *Proceedings of the National Academy of Sciences*. 90:3569-3573.
- Jouiaei M., Yanagihara A. A., Madio B., Nevalainen T. J., Alewood P. F., Fry B. G.. (2015) Ancient Venom Systems: A Review on Cnidaria Toxins. *Toxins*. 7:2251-2271.
- Kass-Simon G., Scappaticci A. A. Jr.. (2002) The Behavioral and Developmental Physiology of Nematocysts. *Canadian Journal of Zoology*. 80(10):1772-1794.
- Kemeny D. M., Dalton N., Lawrence A. J., Pearce F. L., Vernon C. A.. (1984) The Purification and Characterization of Hyaluronidase from the Venom of the Honey Bee, *Apis mellifera*. *European Journal of Biochemistry*. 139:217-223.
- Kemparaju K., Girish K. S.. (2006) Snake Venom Hyaluronidase: a Therapeutic Target. *Cell Biochemistry & Function*. 24:7-12.
- Kim E., Goren A., Ast G.. (2007) Alternative Splicing: Current Perspectives. *Bioessays*. 30(1):38-47.
- Lee H., Jung E., Kang C., Yoon W. D., Kim J., Kim E.. (2011) Scyphozoan Jellyfish Venom Metalloproteinases and their Role in the Cytotoxicity. *Toxicon*. 58:277-284.
- Long-Rowe K. O., Burnett J. W. (1993). Characteristics of Hyaluronidase and Hemolytic Activity in Fishing Tentacle Nematocyst Venom of *Chrysaora quinquecirrha*. *Toxicon*, 32:165-174.
- Mahillon J. and Chandler M.. (1998) Insertion Sequences. *Microbiology and Molecular Biology Reviews*. 62:725-774.
- Mariottini G. L., Pane L. (2010) Mediterranean Jellyfish Venoms: A Review on Scyphomedusae. *Marine Drugs*. 8:1122-1152.
- Mariottini G. L., Pane L. (2014) Cytotoxic and Cytolytic Cnidarian Venoms. A Review on Health Implications and Possible Therapeutic Applications. *Toxins*. 6:108-151.
- Markovic-Housley Z., Miglierini G., Soldatova L., Rizkallah P. J., Müller U., Schirmer, T..(2000) Crystal Structure of Hyaluronidase, a Major Allergen of Bee Venom. *Structure*. 8:1025-1035.
- Meredith R. W., Gayor J. J., Bologna P. A. X.. (2016) Diet assessment of the Atlantic Sea Nettle *Chrysaora quinquecirrha* in Barnegat Bay, New Jersey, using next-generation sequencing. *Molecular Ecology*. 25(24):6248-6266.
- Mount S. M.. (1982) A catalogue of splice junction sequences. *Nucleic Acids Research*. 10(2):459-472.
- Oppgaard S. C., Anderson P. A., Eddington D. T. (2009) Puncture Mechanics of Cnidarian Cnidocysts: a Natural Actuator. *Journal of biological engineering*. 3(17):1-11.
- Özbek S., Balasubramanian P. G., Holstein T. W. (2009) Cnidocyst Structure and the Biomechanics of Discharge. *Toxicon*. 54:1038-1045.
- Piraino S., Boero F., Aeschbach B., Schmid V.. (1996) REverseing the Life Cycle: Medusae Transforming into Polyps and Cell Transdifferentiation in *Turritopsis nutricula* (Cnidaria, Hydrozoa). *The Biological Bulletin*. 190(3):302-312.

- Shinzato C., Shoguchi E., Kawashima T., Hamada M., Hisata K., Tanaka M., Fuije M., Fujiwara M., Koyanagi R., Ikuta T., Fujiyama A., Miller D. J., Satoh N. (2011) Using the *Acropora digitifera* genome to understand coral responses to environmental change. *Nature*. 476:320-323.
- Sievers F., Wilm A., Dineen D., Gibson T. J., Karplus K., Li W., Lopez R., McWillan H., Remmert M., Söding J., Thompson J. D., Higgins D. G.. (2011) Fast, scalable generation of high-quality proteins multiple sequence alignments using Clustal Omega. *Molecular Systems Biology*. 7:539.
- Smith M. M. and Ghosh P.. (1987) The synthesis of hyaluronic acid by human synovial fibroblasts is influence by the nature of the hyaluronate in the extracellular environment. *Rheumatol Int*. 7(3):113-122.
- Stern R., Jedrzejewski M. J. (2006) The Hyaluronidases: Their Genomics Structures, and Mechanisms of Action. *Chem Rev*. 106:818-839.
- Sugahara K., Yamada S., Sugiura M., Takeda K., Yuen R., Khoo H. E., Poh C. H.. (1992) Identification of the Reaction Products of the Purified Hyaluronidase from Stonefish (*Synanceja horrida*) Venom. *Biochemichal Journal*. 283:99-104.
- Suput D. (2009) In Vivo Effects of Cnidarian Toxins and Venoms. *Toxicon*. 54:1190-1200.
- Tibballs J.. (2006) Australian Venomous Jellyfish, Envenomation Syndromes Toxins and Therapy. *Toxicon*. 48:830-859.
- Winnepenninckx, B., Backeijau, T., DeWachter, R. (1993) Extraction of High Molecular Weight DNA from Molluscs. *Trends in Genetics*. 9:407.

Word List #1

Cell Theory
Robert Hooke
Antoine van Leeuwenhoek
Spontaneous Generation
Francesco Redi
Biogenesis
John Needham
fermentation and putrefaction
Lazzaro Spallanzani
Louis Pasteur
abiogenic system
Swan-necked Flasks
John Tyndall
heat labile
heat-resistant
spore (endospore)
autoclave
aseptic technique
neutrons
protons
element
isotope
radioactivity
electrons
ion
electron shells
covalent bond
ionic bond
anabolic
catabolic
enzyme
catalyst
substrate
active site
activation energy
Water
protein
carbohydrates (sugars)
lipids (fats)
DNA
RNA
prions
viroids

viruses
procaryotes
eucaryotes
nanometer
micrometer
millimeter
flagellum
membrane
cell wall
nucleus
organelle
bacterial chromosome
ribosome
golgi
mitochondria
endoplasmic reticulum
chloroplast
lysosome
symbiotic relationship
endocymbiotic evolution
capsid
envelope
spikes
helical virus
polyhedral virus
bacteriophage
bacteria
cocci
bacilli
plasma membrane
simple diffusion
facilitated diffusion
osmosis
active transport
cytoplasm